GEOSEA V Proceedings Vol. II, Geol. Soc. Malaysia, Bulletin 20, August 1986; pp. 423–471

Tin-Tungsten Mineralized Granite at Mae Chedi Area, Wiang Pa Pao District, Chiang Rai Province, Northern Thailand.

R. HANSAWEK[1], W. PONGSAPICH[2] and S. VEDCHAKANCHANA[2]
[1]Economic Geology Division, Department of Mineral Resources,
Bangkok 10400, Thailand
[2]Department of Geology, Chulalongkorn University, Bangkok 10500, Thailand

Abstract: The granitic complexes in the Mae Chedi area, Wing Pa Pao district, Chiang Rai province, northern Thailand, comprise two granitic suites. The first, the GM-series, is associated with the known primary tin-tungsten mineralization and composed of fine-grained biotite (GM-1), fine-grained muscovite-bearing biotite (GM-2), and fine- to medium-grained leucocratic (GM-3) granites. The second, the GR-series, is generally referred to as tin-tungsten barren granite. It is composed of porphyritic biotite (GR-1), medium- to coarse-grained biotite (GR-2), and fine- to medium-grained leucocratic (GR-3) granites.

Both granitic series are geochemically calc-alkaline, peraluminous, and S-type granites. However, the GM-series appears to be less silicic than that of the GR-series and is characterized by higher TiO_2, Al_2O_3, Fe_2O_3, FeO, MnO, MgO, CaO, P_2O_5, H_2O^+, Li, F, Sr, Ba, Zr, Sn, W, Cu, Zn, Ni, Ce and lower Rb contents. Relative differences in Na_2O and K_2O contents between the GM-1, GM-2 and the GR-1, GR-2 are not remarkably sharp. However, the GM-3 is notably lower in Na_2O but higher K_2O contents than that of the GR-3. This and petrographic evidences have led to the belief that the GM-3 is the late metasomatic alteration product of the GM-1, whereas the GR-3 is the late magmatic differentiation product of the GR-1.

The primary tin-tungsten mineralizations occur in the area where small granitic plutons of the GM- series intrude metabasite. The tin and tungsten ores are commonly found in/or adjacent to quartz veins and veinlets cutting through the GM-granitic series, and less commonly, in the metabasite. Wall-rock alterations are characterized by K-feldspathization, tourmalinization, chloritization, sericitization, muscovitization and albitization.

INTRODUCTION

Thailand is one of the major sources of the world's tin-tungsten supply. Most of the tin produced comes from placer deposits in the southern peninsula region. In contrast, the tungsten minerals are mainly produced from primary ore deposits in the northern, central, and southern parts of the country.

The major tin and tungsten deposits of Thailand have a close spatial association with granitic rocks and usually occur near their contacts either within marginal zones of the plutons or in the adjacent intruded country rocks. The tin associated granites of S.E. Asia have been grouped into three belts (Figure 1) namely the eastern, the central, and the western belts (Mitchell, 1977; Hutchison, 1978; Beckinsale, 1979; Mahawat, 1982; Nakapadungrat, 1982).

The Mae Chedi area (Figure 2) is situated in the eastern margin of the N-S trending mountain range that lies on the south-western margin of the Wiang Pa Pao flood plain, southern portion of Wiang Pa Pao district, Chiang Rai province. The Mae

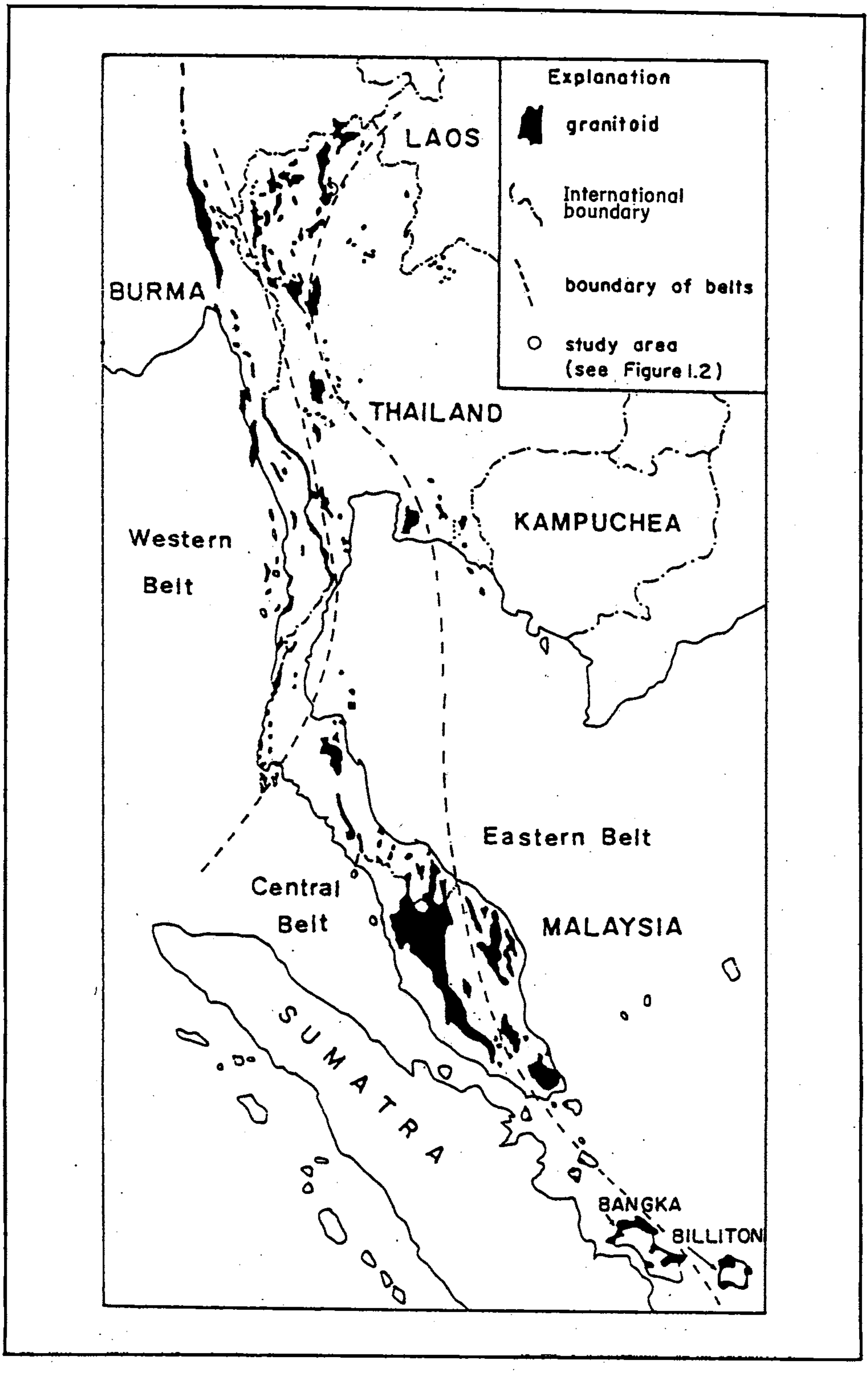

Fig. 1. Sketch map showing the distribution of granitoids in the tin belt of S.E. Asia (compiled after Mitchell, 1977; Hutchison, 1978; Beckinsale, 1979; Mahawat, 1982; Nakapadungrat, 1982).

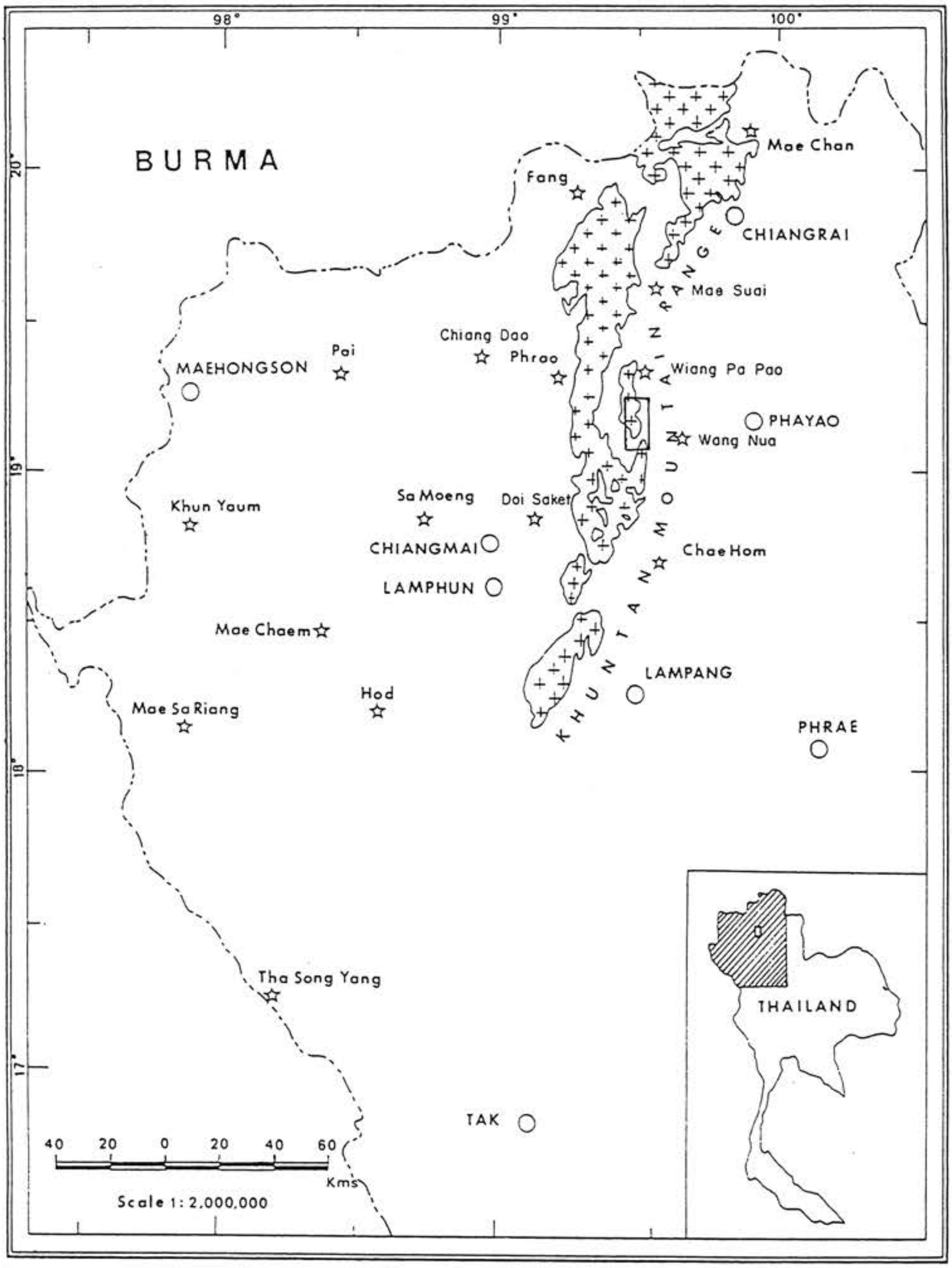

Fig. 2. Index map of northern Thailand showing the location of the study area.

Chedi Mine, a mine for tin and tungsten located near the southern end of the area, is chosen to be an area of interest for this study. The Mae Chedi Mine has close spatial and genetic association with the granitic rocks. The Mae Chedi granites belong to the northernmost portion of the central belt.

The purpose of this study is to characterize in detail the mineralogy, petrology and geochemistry of the Mae Chedi granites and their relation to tin-tungsten mineralization. It is hoped that discovery of certain petrochemical criteria may possibly be employed in delineating targets of potential mineralization. This will contribute a great deal to the geological knowledge not only to mineral exploration in the study area but also elsewhere in Thailand and possibly in other countries.

Method of Investigation

Field mapping and sampling were carried out during late 1980 and mid 1981. The topographic map scale 1:50,000 and modified topographic map scale 1:500 of the Mae Chedi Mine were used as base maps. The aerial photographs were also used to guide the ground survey mapping and to delineate the regional and structural geology of the study area.

The mineralogy and texture of rock samples were studied petrographically. Plagioclase composition was determined by the *a*-normal sections. The optic angle (2V) of K-feldspar was determined by using a universal stage. Staining techniques applying the method modified after Ruperto *et al.* (1964, cited in Hutchison, 1974), Reid (1969), and Norman (1974) have been used to facilitate the mineral grain counting in rock slabs and thin sections. The traverses for thin sections were made on the area of 16 mm by 25 mm, and were spaced 0.33 mm and 0.4 mm apart. The modal composition of the rocks was obtained on the total 3000 point-counts. The traverses for rock slabs were made on the area of 10 cm by 10 cm, with spacing grids of 0.2 cm. The mode was obtained on the total of 2000 point-counts.

At least 1.5 kg of fresh granite and metabasite samples were crushed into small pieces of less than 1 cm in diameter. All crushed samples, after removal of weathered and stained chips, were later carefully detected by short wave ultraviolet light to avoid scheelite contamination. Sampling by the method of quartering was used before pulverization in a tungsten carbide vessel. For samples to be analysed for tungsten content, a chrome-steel vessel was used instead. The powders were mixed well and stored in small glass bottles. Prior to further analyses, all sample powders were dried in an oven at 110°C for 1.5 hours.

All major element-oxide analyses except for H_2O^+ were carried out at the Department of Geology, Chulalongkorn University. H_2O^+, S, Li, F, Sn, W, Cu, Pb, Zn, and Ni were analyzed by the staff of the Chemistry Section, Geological Survey Division, Department of Mineral Resources. Rb, Sr, Ba, Zr, La, Ce, and U were analyzed by the staff of the Physics Division, Office of Atomic Energy for Peace.

The chemical analyses of the rocks have been determined by using several different methods as shown in Table 1.

Table 1

METHODS USED FOR QUANTITATIVE DETERMINATION OF ELEMENTS.

Element	Method
SiO_2, TiO_2, Al_2O_3, total Fe_2O_3	Spectrophotometry
MnO, P_2O_5	Spectrophotometry
FeO	Volumetry
MgO, CaO, Na_2O, K_2O	Atomic Absorption Spectrometry
H_2O^+	Modified Penfield Method
S	Gravimetry
Li, Sn, Cu, Pb, Zn, Ni	Atomic Absorption Spectrometry
F	Ion selective electrodes
Rb, Sr, Ba, Zr, La, Ce	X-ray fluorescence
W	Spectrophotometry
U	Neutron activation analysis

N.B. Fe_2O_3 was calculated from total Fe_2O_3 and FeO by using the relationship: % Fe_2O_3 – (FeO × 1.1113).

GEOLOGY

Regional Geologic Setting

The Khuntan Mountain Range (Figure 2) is mainly occupied by complex granitoids. The range elongates approximately in the N-S direction and extends for a total distance of approximately 250 km. The maximum width across this elongated granitic body is about 45 km.

Rocks of the Khuntan Mountain Range are generally medium- to coarse-grained porphyritic biotite granites and their derivatives, e.g. pegmatites, aplites, and hydrothermal quartz veins. The granitic rocks are Triassic in age, 206 ± 4 Ma, 199 ± 4 Ma, 202 ± 5 Ma (Teggin, 1975), 232 ± 31 Ma (Braun *et al.*, 1976), 212 ± 12 Ma (Beckinsale, 1979), and 215 ± 3 Ma (Nakapadungrat, 1982). They intrude rocks of Palaeozoic sequences ranging from Silurian to Carboniferous. It is evidenced by sharp contacts between the granites and the country rocks in many places (Vichit, 1971, 1973, 1976; Teggin, 1975; Braun *et al.*, 1976; Baum and Hahn, 1977; Suensilpong *et al.*, 1977; Chuaviroj *et al.*, 1978; Gebert *et al.*, 1980; Udomratn *et al.*, 1980).

The following descriptions of the regional geologic setting are summarized from Charoenprawat *et al.* (1980) and Gebert *et al.* (1980) unless otherwise specified. The Silurian-Devonian rocks are exposed on both flanks of the Khuntan Mountain Range. They consist predominantly of schist, phyllite, quartzite, and metamorphosed volcanic rocks of mafic composition. The thickness of the succession is estimated to be in the order of 500–1,000 m near Wiang Pa Pao (Chuaviroj *et al.*, 1978). This metamorphic unit is overlain by nonmetamorphosed Permo-Carboniferous rocks. Rocks of Permo-Carboniferous age outcrop at the south of Mae Chan and the west-southwest of Chiang Rai. They consist of alternating layers of reddish shale, sandstone, conglomerate, tuffaceous shale and sandstone and agglomerates. The Permian limestone of the Ratburi Group is located in the northwest-southwest of Chiang Rai. The thickness of the limestone formation exceeds 100 m.

Felsic volcanic rocks suggested to be of Permo-Triassic age (Udomratn *et al.*, 1980) are found in the northwestern Mae Chan area. Diabase dikes, found along Nam Mae Ko, northeast of Wiang Pa Pao, intrude the Silurian-Devonian metamorphic complex in the NE direction. The rocks were suggested to be of Tertiary age (Chuaviroj *et al.*, 1978).

Quaternary sediments are found in the north and the southwest of Chiang Rai and in the Nam Mae Lao Valley. The unconsolidated clastic sediments consist mainly of gravel, sand, and clay of Pleistocene age (Baum, *et al.*, 1970).

Geology of the Mae Chedi Area

Geologic map of the Mae Chedi area is illustrated in Figure 3. The study area is situated on the east-central part of the Khuntan Mountain Range. It is covered predominantly by intrusive rocks of granitic compositions. The oldest rocks in the study area consist of various metasediments, namely, schist, phyllite, and quartzite, and meta-mafic volcanics (metabasites) of probable Silurian-Devonian age (Charoenprawat *et al.*, 1980; Gebert *et al.*, 1980). These rocks have been intruded by the N-S elongated body of the presumably Triassic granites throughout the area.

Metamorphic rocks of the Silurian-Devonian age are exposed in southeast and southwest of the area. They are generally grouped as being metamorphic rocks of the greenschist facies. Phyllite and schist are more abundant than quartzite (Gebert *et al.*, 1980). These metasediments have been folded with the fold-axes in the N-S to NE-SW directions (Charoenprawat *et al.*, 1980).

The metabasites were previously called "basic volcanic rocks" (Baum and Hahn, 1977; Charoenprawat *et al.*, 1980; Gebert *et al.*, 1980) and "ophiolite" (Baum *et al.*, 1970) for field description purposes. According to German Geological Mission (1972), they are mainly andesites and pyroxenites of Late Carboniferous age. They are interpreted to be a result of volcanic activity in a geosynclinal environment (Gebert *et al.*, 1980).

Granites are the most abundant rocks throughout the study area. On the basis of field observations, they can be classified into six types, namely:

1. Fine-grained biotite granite (GM-1)
2. Fine-grained muscovite-bearing biotite granite (GM-2)
3. Fine- to medium-grained leucocratic granite (GM-3)
4. Porphyritic biotite granite (GR-1)
5. Medium- to coarse-grained biotite granite (GR-2)
6. Fine- to medium-granied leucocratic granite (GR-3)

The rock types mentioned above can be grouped into two series. The GM-series, collected from the immediate Mae Chedi Mine (GM-1 to GM-3) (Figure 4) are

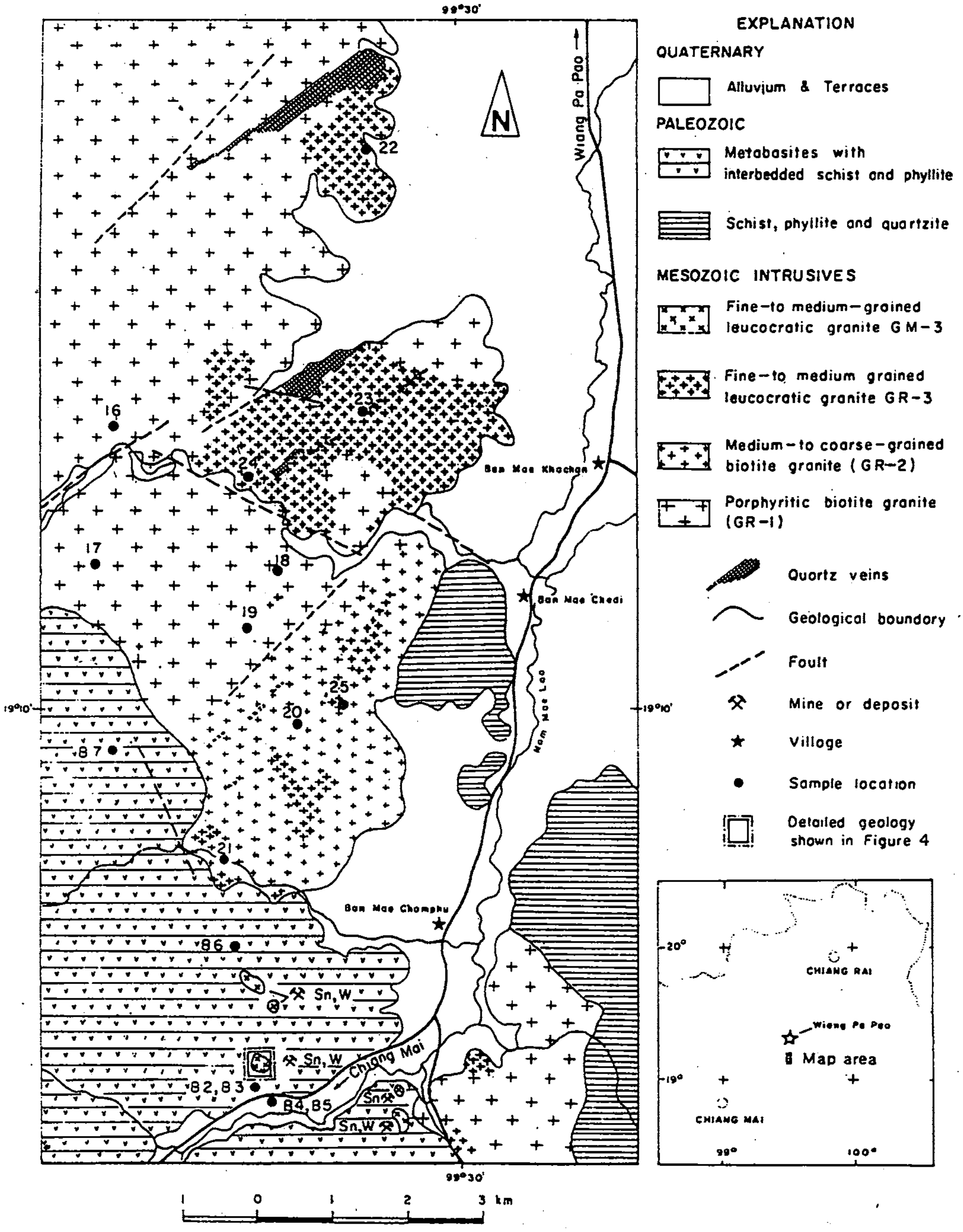

Fig. 3. Geologic map of the Mae Chedi area, Wiang Pa Pao, Chiang Rai (modified after Gebert *et al.*, 1980).

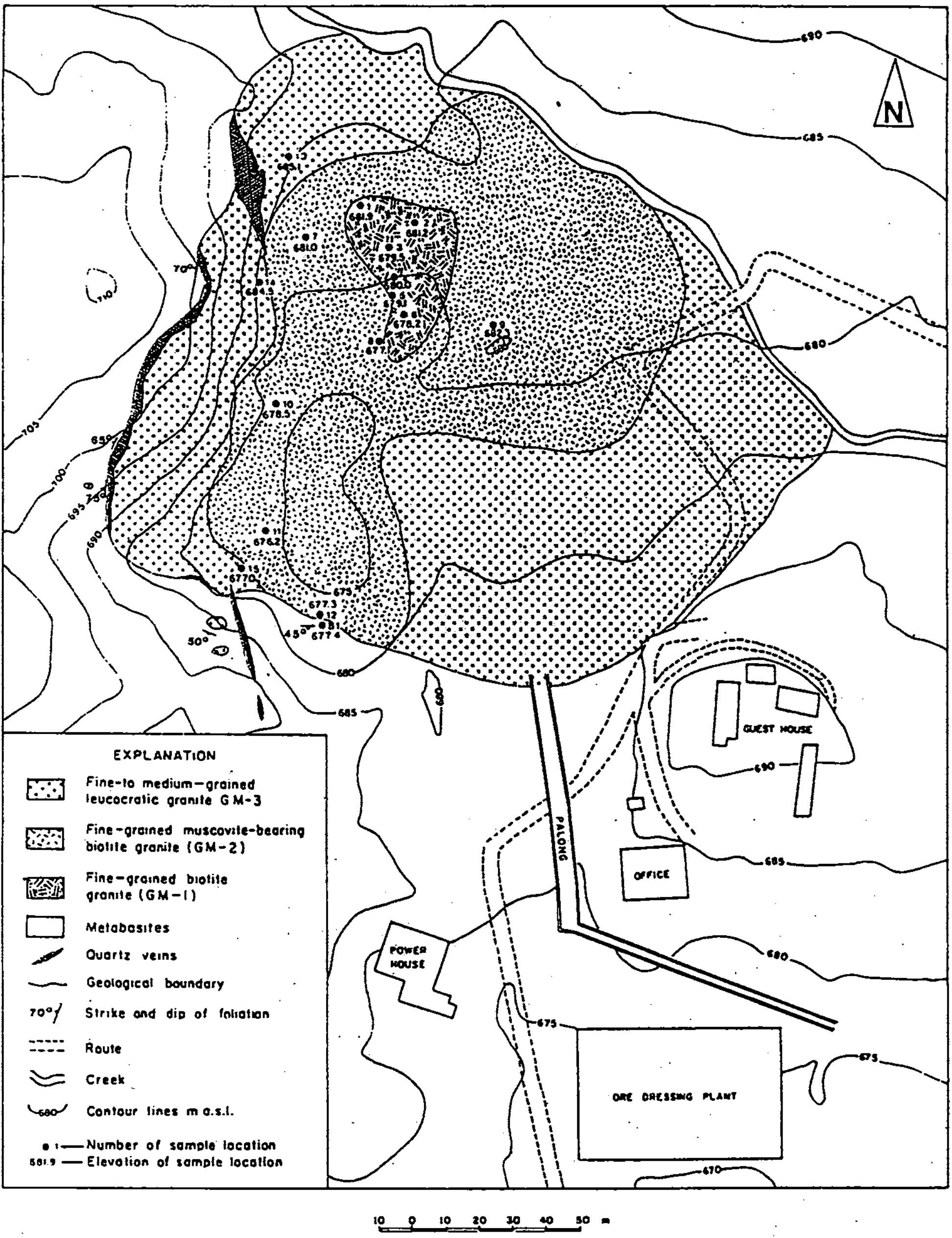

Fig. 4. Geologic map of the Mae Chedi Sn-W Mine, Wiang Pa Pao, Chiang Rai.

associated with tin-tungsten mineralization. The GR-series were collected from outside the Mae Chedi Mine (GR-1 to GR-3). To the author's knowledge the latter series are normally tin-tungsten barren. Distribution and sample locations of the GM- and the GR-series are shown in Figures 3 and 4.

The primary tin-tungsten mineralization is found where a small granitic pluton intrudes the metabasites. The granitic pluton appears to be a small cupola covering an area of approximately 0.5 km^2 (Figure 4). The granitic rock is in sharp contact with metabasites and possesses internal vertical and lateral zonations. It is a fine-grained biotite granite (GM-1) in the core area and transitionally grades outward into fine-grained muscovite-bearing biotite granite (GM-2) and finally to fine- to medium-grained leucocratic granite (GM-3) in the marginal zone.

The ore bodies commonly occur in quartz veins cutting through the granites and less commonly in metabasites. The widths of ore bearing veins vary from a few mm up to 50 cm. They are entirely fracture-controlled. The major ore-bearing veins systems are predominant in the N-S direction. The stereogram plot and rose diagram of 318 measurements of fractures recorded in this granitic pluton are shown in Figure 5.

Mineral constituents of ore-bearing veins are very variable. The major ore minerals are scheelite and cassiterite. However, wolframite frequently rimmed by scheelite have been found in quartz veins cutting through the GM-1 granitic rock. Gangue minerals comprise predominantly of quartz, tourmaline, chlorite, pyrite, chalcopyrite and to a minor extent of arsenopyrite. Occurrences of disseminated ores are also observed. They are generally restricted to the wall rocks adjacent to ore-bearing veins.

It is interesting to note from the present field observation that there is an apparent zonation of metallization in the deposit. Occurrences of cassiterite are chiefly associated with the GM-3 granitic rock, especially in the apical zone of the cupola, whereas scheelite is commonly abundant toward the lower level particularly in the GM-2 granitic type.

PETROGRAPHY

Granitic Rocks

25 modal analyses of the Mae Chedi granites were determined and are presented in Table 2. The amount of the combined quartz and feldspars (felsic minerals) constitute well over 90 percent of the total mineral constituents. It is clearly seen that the average felsic mineral contents progressively increase both from the GM-1, the GM-2 to the GM-3 and from the GR-1, the GR-2 to the GR-3. It is important to note that the contrasting feature of the felsic minerals between the GM- and the GR-granitic series is their feldspar content as illustrated in Table 2. In the GM- granitic series, plagioclase is the most abundant phase in the GM-1 and GM-2 then its quantity remarkably declines in the GM-3 whilst K-feldspar is the least abundant among the felsic constituents in the GM-1 which then become numerous in the GM-2 and it is most widespread in the GM-3. In contrast, a comparative abundance of plagioclase and K-feldspar in the GR-granitic series is the reverse of the GM-granitic suites (Figure 6).

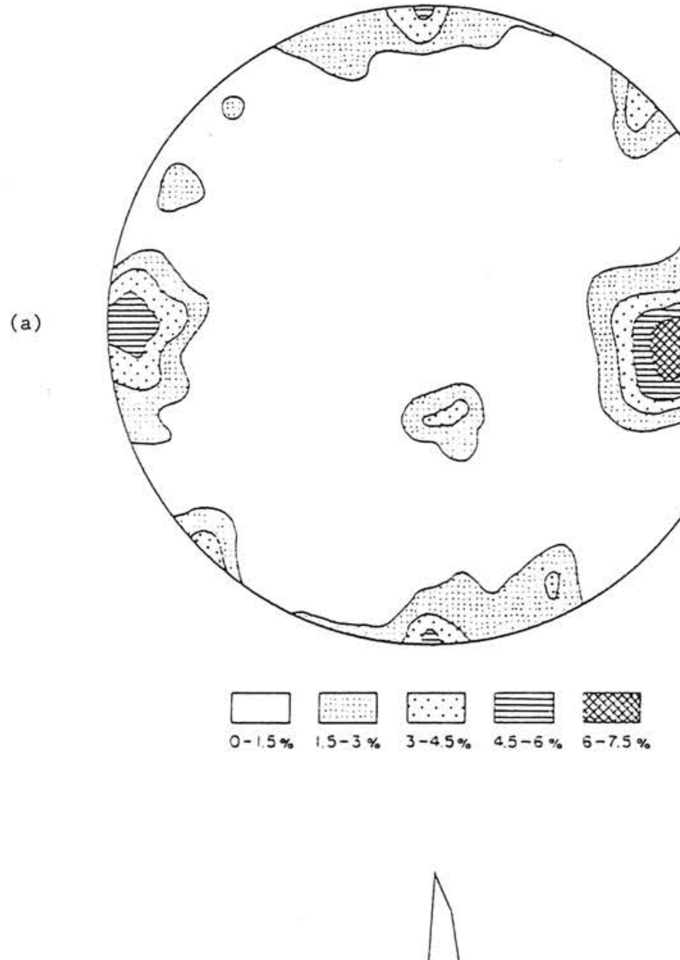

Fig. 5. Patterns of fracture distribution in granite rock of the Mae Chedi Sn-W Mine.

(a) Distribution illustrated in an equal-area stereographic net plot of 318 poles of fractures (joints and faults).

(b) Distribution of strike of 318 fractures illustrated by a rose diagram.

TABLE 2

MODAL ANALYSES OF THE MAE CHEDI GRANITES (VOLUME %)

Sample No. (Grid Reference)	Rock Type	O	Kf	Pl	An-Content in Pl	Bi	ChBi	Mus	Op	Others	Staining Sample
(1) M1–13 (499145)	GM–1	27.34	18.27	37.73	An_{34} $(An_{27}–An_{45})$	13.80	1.43	N.D.	0.90	0.53	thin section
(2) S–4B (499145)	GM–1	30.00	25.60	30.83	An_{33}	10.07	3.07	N.D.	0.30	0.13	thin section
(3) S–3 (499145)	GM–1	30.30	28.07	31.23	An_{30}	5.37	3.73	0.10	1.07	0.13	thin section
(4) M1–12 (499144)	GM–1	29.90	18.20	35.37	An_{35}	14.97	1.00	N.D.	0.43	0.13	thin section
(5) M1–11–2 (499144)	GM–1	31.80	25.83	31.57	An_{31}	7.77	0.47	1.10	0.73	0.73	thin section
(6) S–2 (499144)	GM–1	26.24	21.40	35.23	An_{38}	14.67	0.43	N.D.	1.00	1.03	thin section
(7) M1–18 (498145)	GM–2	33.87	23.20	34.30	An_{14}	2.63	2.90	2.33	0.53	0.23	thin section
(8) M1–11 (499144)	GM–2	28.87	30.97	34.19	An_5	1.97	3.23	0.03	0.67	0.07	thin section
(9) M1–15 (499144)	GM–2	28.50	32.23	32.87	An_7	0.80	4.34	0.13	0.60	0.53	thin section
(10) M1–9 (498144)	GM–2	26.57	38.27	30.50	An_{12}	1.66	1.93	0.43	0.37	0.27	thin section
(11) M1–7 (498143)	GM–2	27.37	28.70	36.10	An_5	0.56	5.20	0.63	1.17	0.27	thin section
(12) M1–4B (498143)	GM–2	28.53	29.87	35.47	An_7	N.D.	4.93	0.03	1.00	0.17	thin section
(13) M1–24 (498145)	GM–3	31.03	33.54	29.23	An_2	N.D.	1.73	3.50	0.80	0.17	thin section
(14) M1–23 (498144)	GM–3	26.90	41.23	26.17	An_2	N.D.	1.57	3.57	0.33	0.23	thin section
(15) M1–6 (498143)	GM–3	30.20	30.62	34.42	An_1	N.D.	1.68	1.88	0.98	0.22	thin section

TABLE 2—CONTINUED

Sample No. (Grid Reference)	Rock Type	Q	Kf	Pl	An-Content in Pl	Bi	ChBi	Mus	Op	Others	Staining Sample
(16) MD 11 (480229)	GR–1	39.10	33.87	19.88	An_{28} $(An_{23}–An_{33})$	6.40	n/d	0.60	N.D.	0.15**	rock slab
(17) MD 10 (478210)	GR–1	31.18	39.93	20.82	An_{36}	8.07	n/d	N.D.	N.D.	N.D.	rock slab
(18) MD 6 (502209)	GR–1	33.48	39.78	19.70	An_{32} $(An_{12}–An_{55})$	6.62	n/d	0.42	N.D.	N.D.	rock slab
(19) MD 7 (497202)	GR–1	35.43	31.48	24.18	An_{34} $(An_{13}–An_{55})$	8.91	n/d	N.D.	N.D.	N.D.	rock slab
(20) MD 22 (504189)	GR 2	37.03	32.60	26.10	An_{13}	2.07	0.90	0.60	0.57	0.13	thin section
(21) MD 24 (494171)	GR–2	33.53	40.31	21.53	An_{35}	3.98	n/d	0.13	N.D.	0.52**	rock slab
(22) MD 35 (494171)	GR–3	34.50	31.93	32.34	An_{14}	0.63	0.30	N.D.	0.30*	N.D.	thin section
(22) MD 35 (514267)	GR–3	34.50	31.93	32.34	An_{14}	0.63	0.30	N.D.	0.30*	N.D.	thin section
(23) MD 16 (513232)	GR–3	36.03	31.90	31.66	An_{7}	N.D.	0.10	0.27	0.3*	N.D.	thin section
(24) MD 13 (498222)	GR–3	36.07	30.57	32.53	An_{10}	N.D.	0.10	0.30	0.43*	N.D.	thin section
(25) MD 21 (510193)	GR–3	38.63	26.27	31.20	An_{7}	N.D.	0.13	1.70	0.07*	2.00**	thin section

Abbreviations: Q = quartz, Kf = potassium feldspar, P1 = plagioclase, Bi = biotite, ChBi = chloritized biotite, Mus = muscovite, Op = opaque minerals including iron oxides, pyrite, chalcopyrite and arsenopyrite, *iron oxides only, Others including apatite, zircon, sphene, chlorite, and tourmaline (plus scheelite in sample (15) M1–6), ** tourmaline only, N.D. = not detected, n/d = not determined.

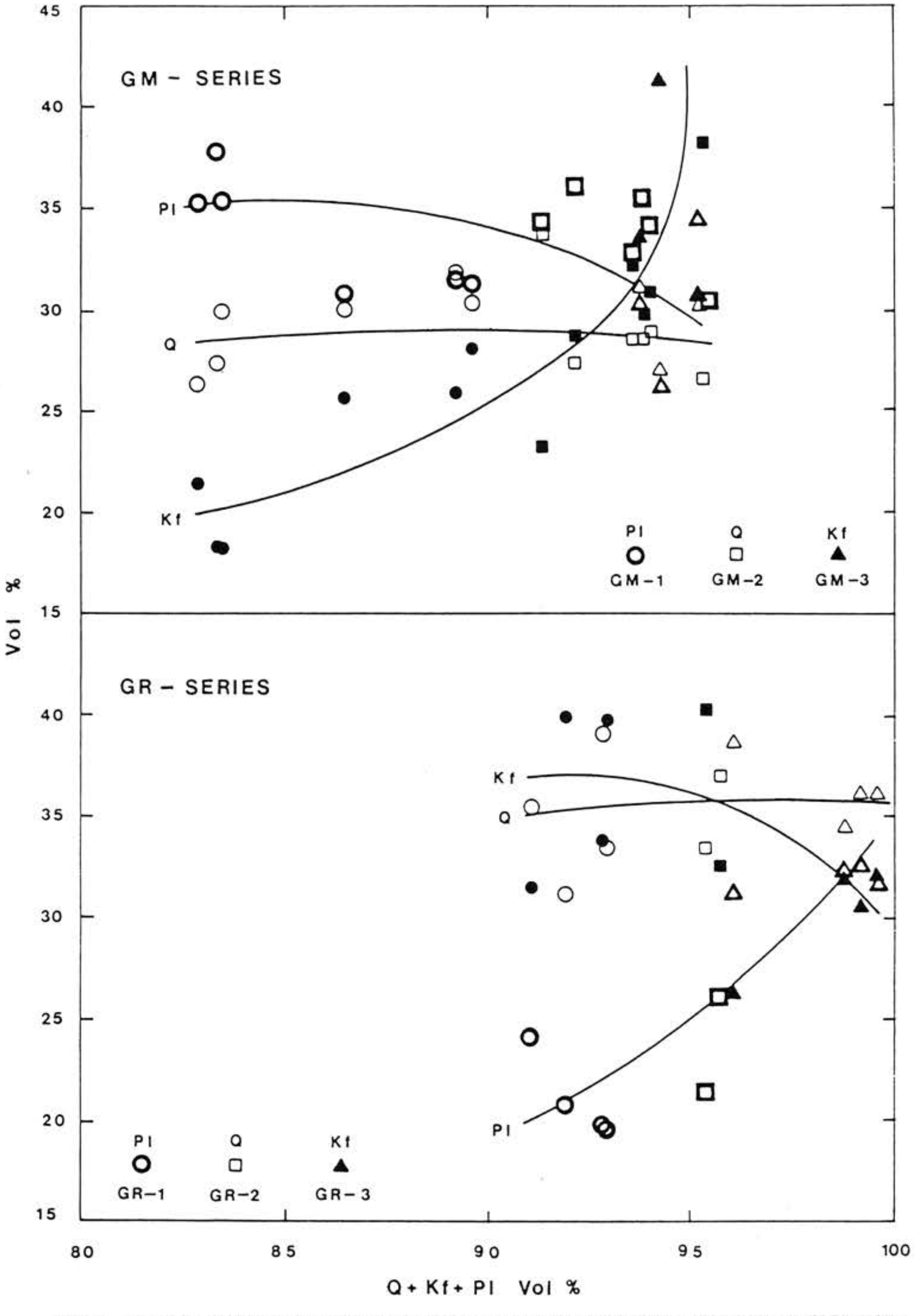

Fig. 6. Variation of the modal abundance of plagioclase (P1), quartz (Q), and K-feldspar (Kf) against felsic minerals (Q + Kf + P1) for the Mae Chedi granites.

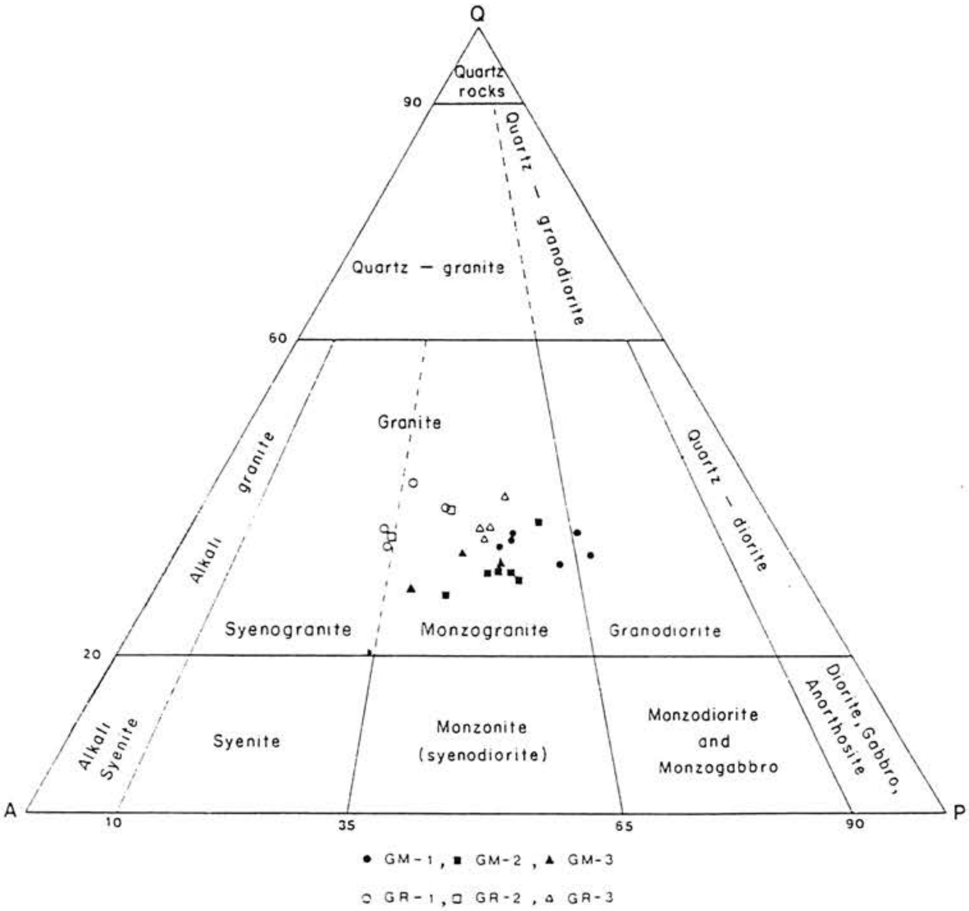

Fig. 7. Modal quartz, alkali feldspar and plagioclase of the Mae Chedi granites plotted in the plutonic rock classification diagram after Streckeisen (1976).

The modal abundance of quartz, K-feldspar, and plagioclase, is plotted on a triangular diagram (Figure 7) for the classification of plutonic rocks proposed by Streckeisen (1976). The diagram shows that almost all of the Mae Chedi granites fall within the granite field boundary particularly monzogranite region. It is apparent that the evolution trend of the GM-granitic series is characterized by decreasing and increasing amounts of plagioclase and K-feldspar respectively. On the other hand, the evolution trend of the GR-granitic series is characterized by the increase of plagioclase and decrease of K-feldspar. Thus, it can be concluded that the granite which may have given rise to Sn-W mineralization, at the Mae Chedi area is characterized by high K-feldspar content. A similar conclusion was also obtained from the studies of granites in the vicinity of tin-tungsten mining area at Samoeng, northern Thailand (Puyaprasiddhi, 1980). In contrast, it is interesting to note that the Sn-W-bearing granite at Haad Som Pan, Ranong, southern Thailand is characterized by low K-feldspar content (Aranyakanon, 1961).

Fine-grained biotite granite (GM-1)

The rock is generally dark-grey, fine-grained and subequigranular. Under the microscope, the rock exhibits a sequence of crystallization of major mineral constituents as biotite, plagioclase, quartz, and microcline. Biotite is the only essential mafic mineral and partially altered to chlorite. Plagioclase (An_{30-38}) is the most abundant constituent of the rock. Normal zoning is common feature of plagioclase which is characterized by calcic andesine in the core and calcic oligoclase at the margins. Most of the plagioclase crystals appear to be intensely sericitized especially in the core. Quartz seems to be crystallized just before K-feldspar. Microcline forms large tabular poikilitic phenocrysts as well as small interstitially anhedral grains filling in the intergranular spaces between formerly crystallized mineral aggregates.

Accessory minerals are muscovite, apatite, zircon, tourmaline, and opaques. Secondary minerals are muscovite, chlorite, and sphene.

Fine-grained muscovite-bearing biotite granite (GM-2)

This rock is generally similar to the GM-1 with respect to its mineral constituents, sequence of crystallization, and, in particular, textures. Major differences between them are, in the GM-2, the average total content of felsic minerals sharply increases and biotite decreases. The increase in the average total felsic mineral in the GM-2 is actually reflected by the addition of K-feldspar alone since the numbers of quartz and plagioclase remain relatively the same. Biotite (often chloritized) and minor muscovite are the main characteristics of this rock type and they make the rock light greenish grey in colour. Alteration in the GM-2 appears to be more extensive than that of the GM-1. It is characterized by K-feldspathization, chloritization, sericitization, muscovitization, tourmalinization, and albitization. Zoning texture in many plagioclase (An_{5-14}) grains is obscured by this intensive alteration. Quartz has been crystallized before alkali feldspar and lasted till the final liquid.

Microline is usually perthitic and forms large tabular poikilitic grains as well as small anhedral patches replacing the host plagioclase.

Accessory minerals include apatite, zircon, sphene, tourmaline, iron oxides, pyrite, chalcopyrite and arsenopyrite.

Fine- to medium-grained leucocratic granite GM-3

The term "leucocratic granite" (including the GR-3) used herein is characterized by its white colour due to the trace or small amounts of mafic minerals.

The GM-3 granite is mostly fine-grained. However, medium-grained varieties (grain size up to 2 mm) are also present, especially near the upper level of the pluton. Some K-feldspar crystals, as large as 4 by 6 mm, make the rock slightly porphyritic in appearance.

Biotite is the least abundant major mineral and is represented by a small amount of relic chloritized biotite. Plagioclase is relatively less abundant compared with that of other rock types in the GM-series. Almost all plagioclase grains show intensive sericitization. The composition of plagioclase is surprisingly almost pure albite (An_{1-2}). This leads the authors to conclude that the GM-3 is the ultimate albitization of the GM-granitic series. Quartz occurs both as large anhedral patches and as small interstitial aggregates. Most of them show strained effects. Microcline is numerous, typically as late interstitial anhedral patches and replacing plagioclase. Obviously, it is the most abundant constituent of the GM-3 granitic rock.

Muscovite is present in substantial amounts. It is believed that the GM-3 is the ultimate alteration product of the GM-1 resulting in a drastic increment of the muscovite content. All of the accessory minerals that have been recognized in the GM-1 and the GM-2 are also commonly present in the GM-3. Occasionally, small anhedral scheelite grains (up to 1 mm) have been spatially associated with albitic plagioclase. In addition, minute scheelite grains are enclosed in plagioclase.

Porphyritic biotite granite (GR-1)

This granite is the most abundant type and is widely distributed throughout the study area. The rock is generally light grey to grey, porphyritic, with medium-grained groundmass (1–5 mm) and with phenocrysts of K-feldspar ranging in size from 1 by 2 cm to 3 by 6 cm (usually 1 by 2 to 1 by 3 cm). Mineral constituents of the groundmass, in a sequential order of crystallization, are biotite, plagioclase, K-feldspar, and quartz.

Biotite occurs as clusters of flakes as well as individual grains. It is partially altered to chlorite. Plagioclase (An_{8-36}) generally shows subhedral grains of varying sizes ranging from 2 to 5 mm. Normal zoning in plagioclase is common. The core is calcic andesine or sodic labradorite whereas the rim is sodic to intermediate oligoclase (see Table 2). Quartz occurs mostly as interstitial anhedral grains of late crystal aggregates. Strained quartz with undulose extinction is commonly observed. Microcline appears to be the most abundant mineral of the rock. It is the only phenocrysts with subhedral shape. K-feldspar also occurs as anhedral grains in the groundmass. The phenocrysts usually show poikilitic texture containing biotite, plagioclase, and occasionally, apatite. Carlsbad twin is frequently found especially in the phenocrysts, many of which show perthitic textures.

Muscovite is scarce and considered to be a secondary mineral which occurs as small flakes (up to 2 mm) in association with chloritized biotite. Sphene and chlorite are also considered to be secondary minerals. Apatite, zircon, and tourmaline are accessory minerals.

Medium-to coarse-grained biotite granite (GR-2)

The GR-2 is generally similar to the GR-1, particularly in mineralogy, except for its slightly porphyritic texture and considerably lesser biotite content (Table 2). The rock is normally light gray. Its grain size varies from 1 to 10 mm (usually 2 to 5 mm). It has minor K-feldspar phenocrysts, having grain size up to 1 by 2 cm.

Biotite occurs as small discrete flakes (up to 2 mm), many of which are intensely chloritized. The biotite constituents are also remarkably lower than that of the GR-1. Many grains of plagioclase (An_{13-35}) are intensely sericitized especially at their zoned cores. Myrmekitic textures are very common. Quartz occurs both as large anhedral patches and as interstitial grains. Microcline occurs as large subhedral phenocrysts and as anhedral aggregates of smaller grains in the groundmass.

Muscovite occurs in trace amounts and is always in close association with the chloritized biotite. Other accessory minerals are generally similar to those of the GR-1 but notably less abundant. They are apatite, zircon, sphene, chlorite, iron oxides, and tourmaline. All of them are in close association with biotite or chloritized biotite.

Fine- to medium-grained leucocratic granite GR-3

It is white or light greenish white, mostly fine-grained but locally medium-grained, and slightly porphyritic due to scattered occurrences of K-feldspar phenocrysts (up to 3 by 6 mm). By comparing the GR-3 with the GM-3, the former is notably higher in quartz and plagioclase but lower in K-feldspar.

Biotite occurs only in trace amounts. In general, almost all of the biotite grains of this rock type are affected by the process of chloritization. Plagioclase (An_{7-14}) occurs as subhedral crystals and generally lacks zoning. It is intensely sericitized. Quartz forms as late crystallized aggregates and interstitial grains among the earlier crystallized minerals. It commonly shows undulose extinction. Microcline occurs as anhedral crystals and shows interlocking boundaries with quartz and plagioclase. Perthitic textures are also not uncommon.

Muscovite is generally present in trace amounts. It occurs as small patches and is found to be in association with chloritized biotite and opaque minerals. It should be noted that the accessory minerals, i.e. apatite, zircon, sphene and tourmaline are rare in the GR-3.

Metabasites

The rock is greenish black to black, fine-grained, foliated, and durable. The rock locally shows blastoporphyritic texture containing porphyroblasts of amphibole ranging up to a maximum size of 5 by 10 mm. It shows a more or less distinct foliation due to the sub-parallel preferred orientation of the amphiboles and plagioclase.

The major mineral constituents of the rock are hornblende and plagioclase (andesine-labradorite). Common accessory minerals are sphene, chlorite, pyrite, and iron oxide, presumably magnetite. Plagioclase is generally in equant form and locally shows intensive sericitization. Diopside may also be common in certain specimens.

GEOCHEMISTRY

Granitic Rocks

A total of 25 samples of granites from the Mae Chedi Sn-W Mine and its vicinity were chemically analysed for their major and trace element concentrations. Table 3

TABLE 3

MAJOR ELEMENT-OXIDE ANALYSES, CIPW NORMS AND DIFFERENTIATION INDEX (D.I.) OF THE MAE CHEDI GRANITES

Rock Type	GM-1						GM-2	
Sample No.	(1)M1–13	(2)S–4B	(3)S–3	(4)M1–12	(5)M1–11–2	(6)S–2	(7)M1–18	(8)M1–11
Major element oxides (wt.%)								
SiO_2	68.16	70.45	70.59	68.23	71.43	69.23	72.19	73.36
TiO_2	0.54	0.37	0.39	0.52	0.28	0.52	0.25	0.23
Al_2O_3	15.42	14.86	15.06	15.42	14.50	15.42	14.58	13.77
Fe_2O_3	1.51	1.03	1.26	1.22	1.05	1.31	1.04	0.88
MnO	0.09	0.06	0.06	0.10	0.04	0.05	0.03	0.02
MgO	1.91	1.21	1.25	1.88	0.76	1.67	0.61	0.57
CaO	1.39	1.34	1.09	1.76	1.39	1.59	0.95	0.33
Na_2O	2.96	2.71	2.69	2.89	2.94	3.01	3.01	3.23
K_2O	4.26	5.03	4.80	4.03	4.88	4.03	4.76	4.88
P_2O_5	0.18	0.11	0.12	0.18	0.18	0.12	0.19	0.12
H_2O^+	1.51	1.39	1.29	1.25	1.67	1.21	1.03	1.72
Total	99.80	99.82	99.94	99.61	99.88	100.06	99.22	99.60
CIPW norms								
Q	28.66	30.63	32.31	28.92	31.77	30.25	33.86	34.68
or	25.17	29.73	28.36	23.81	28.84	23.81	28.13	28.84
ab	25.05	22.93	22.76	24.46	24.88	25.47	25.47	27.33
an	5.72	5.93	4.62	7.55	6.11	6.65	3.39	0.85
C	3.84	2.78	3.75	3.53	2.14	3.67	3.04	2.86
hy en	4.76	3.01	3.11	4.68	1.89	4.16	1.52	1.42
hy fs	1.46	0.96	0.89	2.23	0.25	1.51	–	–
mt	2.19	1.49	1.83	1.77	1.52	1.90	1.47	0.98
hm	–	–	–	–	–	–	0.03	0.21
il	1.03	0.70	.074	0.99	0.53	0.99	0.47	0.44
ap	0.42	0.25	0.28	0.42	0.28	0.44	0.28	0.28
Salic tot.	88.44	92.00	91.80	88.27	93.74	89.85	94.43	94.56
Femic tot.	9.86	6.41	6.85	10.09	4.47	9.00	3.77	3.33
D.I.	80.2	84.6	84.6	78.5	87.0	80.5	89.1	92.8

TABLE 3-CONTINUED

Rock Type	GM-2				GM-3			GR-1
Sample No.	(9)M1–19	(10)M1–9	(11)M1–7	(12)M1–4B	(13)M1–24	(14)M1–23	(15)M1–6	(16)MD11
Major element oxides (wt.%)								
SiO_2	72.72	72.59	72.90	72.23	74.34	74.72	74.14	73.05
TiO_2	0.23	0.22	0.22	0.30	0.15	0.11	0.14	0.24
Al_2O_3	14.21	14.50	14.26	13.73	14.50	14.21	14.21	14.25
Fe_2O_3	1.00	0.81	0.84	1.42	0.29	0.16	0.35	0.69
FeO	0.43	0.52	0.37	0.72	0.08	0.08	0.10	0.84
MnO	0.02	0.03	0.01	0.03	N.D.	N.D.	N.D.	0.04
MgO	0.57	0.49	0.53	0.86	0.19	0.19	0.20	0.57
CaO	0.47	0.83	0.34	0.48	0.34	0.42	0.34	1.23
Na_2O	2.91	3.02	3.04	3.49	2.59	2.47	2.99	2.96
K_2O	5.53	5.50	5.50	4.25	5.61	5.78	5.50	4.84
P_2O_5	0.11	0.12	0.11	0.13	0.11	0.14	0.10	0.07
H_2O^+	1.49	1.12	1.52	1.78	1.17	1.04	1.66	0.76
Total	99.69	99.75	99.64	99.42	99.37	99.32	99.73	99.54
CIPW norms								
Q	33.08	31.81	32.96	33.72	37.10	37.45	34.96	33.72
or	32.68	32.50	32.50	25.12	33.15	34.16	32.50	28.60
ab	24.62	25.56	25.72	29.53	21.92	20.90	25.30	25.05
an	1.62	3.33	0.97	1.53	0.97	1.17	1.04	5.65
C	2.84	2.36	2.95	2.83	3.81	3.46	2.96	2.07
hy en	1.42	1.22	1.32	2.14	0.47	0.47	0.50	1.42
hy fs	–	–	–	–	–	–	–	0.65
mt	0.78	1.14	0.59	1.55	–	–	–	1.00
hm	0.46	0.03	0.43	0.35	0.29	0.16	0.35	–
il	0.44	0.42	0.42	0.57	0.17	0.17	0.21	0.46
ru	–	–	–	–	0.06	0.02	0.03	–
ap	0.25	0.28	0.25	0.30	0.25	0.33	0.23	0.16
Salic tot.	94.84	95.56	95.10	92.73	96.95	97.14	96.76	95.09
Femic tot.	3.35	3.09	3.01	4.91	1.24	1.15	1.32	3.69
D.I.	92.0	91.1	92.9	90.5	93.9	94.1	94.6	88.4

N.D. = not detected

TABLE 3—CONTINUED

Rock Type	GR-1			GR-2			GR-3		
Sample No.	(17)MD10	(18)MD6	(19)MD7	(20)MD22	(21)MD24	(22)MD35	(23)MD16	(24)MD13	(25)MD21
Major element oxides (wt.%)									
SiO_2	71.65	72.85	73.05	74.34	75.24	76.32	76.32	77.26	76.68
TiO_2	0.35	0.28	0.29	0.22	0.17	0.07	0.06	0.06	0.07
Al_2O_3	14.01	13.65	14.25	13.29	13.65	12.88	13.36	13.12	13.05
Fe_2O_3	0.96	1.06	0.81	0.98	0.92	0.24	TR.	0.33	0.16
FeO	1.23	0.77	1.08	0.58	0.22	0.07	0.05	0.12	0.12
MnO	0.02	0.02	0.02	0.07	0.03	N.D.	N.D.	N.D.	N.D.
MgO	1.04	0.75	0.83	0.49	0.36	0.06	0.03	0.09	0.13
CaO	1.52	1.12	1.31	0.46	0.76	0.68	0.17	0.31	0.21
Na_2O	2.88	2.84	2.67	2.79	3.14	3.23	3.52	3.59	3.09
K_2O	4.65	4.87	4.87	4.98	4.75	4.98	4.91	4.24	5.17
P_2O_5	0.11	0.07	0.09	0.05	0.05	0.01	0.01	0.05	0.05
H_2O^+	1.34	1.06	0.83	1.53	1.14	1.05	0.96	0.59	0.89
Total	99.76	99.34	100.10	99.78	100.43	99.61	99.39	99.76	99.62
CIPW norms									
Q	32.18	34.32	34.69	37.47	36.78	36.96	36.68	39.49	38.42
or	27.48	28.78	28.78	29.43	28.07	29.43	29.01	25.06	30.55
ab	24.37	24.03	22.59	23.61	26.57	27.33	29.78	30.38	26.15
an	6.83	5.10	5.91	1.96	3.44	3.31	0.78	1.21	0.72
C	1.74	1.84	2.42	2.59	2.08	0.96	1.97	2.18	2.11
hy en	2.59	1.87	2.07	1.22	0.90	0.15	0.07	0.22	0.32
hy fs	0.92	0.11	0.87	0.02	–	–	–	–	–
mt	1.39	1.54	1.17	1.42	0.31	0.09	–	0.21	0.19
hm	–	–	–	–	0.70	0.18	–	0.18	0.03
il	0.66	0.53	0.55	0.42	0.32	0.13	0.11	0.11	0.13
ap	0.25	0.16	0.21	0.12	0.12	0.02	0.02	0.12	0.12
Salic tot.	92.60	94.07	94.39	95.06	96.94	97.99	98.22	98.32	97.95
Femic totl.	5.81	4.21	4.87	3.20	2.35	0.57	0.20	0.84	0.79
D.I.	85.4	88.7	86.7	92.1	92.1	95.1	97.0	95.7	96.3

TR. = trace, N.D. = not detected

TABLE 4

TRACE ELEMENT ANALYSES AND ELEMENTAL RATIOS OF THE MAE CHEDI GRANITES

Rock Type	GM-1						GM-2	
Sample No.	(1)M1–13	(2)S–4B	(3)S–3	(4)M1–12	(5)M1–11–2	(6)S–2	(7)M1–18	(8)M1–11
Trace elements (ppm)								
Li	50	38	34	55	36	55	19	15
F	1188	1665	1476	1483	1012	1217	522	463
Rb	401	388	431	364	392	344	387	419
Sr	157	88	68	101	62	117	74	87
Ba	812	527	516	768	565	667	563	555
Zr	176	124	126	155	97	162	109	98
Sn	6.0	6.0	6.5	7.5	10.0	3.0	1.0	17.5
W	15.6	6.9	6.4	7.6	7.6	18.2	6.1	23.3
Cu	60	29	26	60	70	18	28	18
Pb	50	72	68	56	85	68	560*	56
Zn	113	56	77	99	260*	90	278*	38
Ni	38	20	20	40	105*	25	195*	25
La	57	53	43	66	44	69	58	25
Ce	144	91	73	166	80	110	90	58
U	10.5	21.2	22.6	14.1	15.1	13.9	20.2	15.6
Elemental ratios								
K/Rb	88.2	107.6	92.5	91.9	103.4	97.3	102.1	96.7
Ba/Rb	2.0	1.4	1.2	2.1	1.4	1.9	1.5	1.3
K/Ba	43.6	79.2	77.2	43.6	71.7	50.2	70.2	73.0
Rb/Sr	2.6	4.4	6.3	3.6	6.3	2.9	5.2	4.8
Ca/Sr	63.3	108.8	114.6	124.5	160.2	97.1	91.8	27.1
Zr/Sn	29.3	20.7	19.4	20.7	9.7	54.0	109.0	5.6
Zn/Pb	2.3	0.8	1.1	1.8	3.1	1.3	0.5	0.7
F/Li	23.8	43.8	43.4	27.0	28.1	22.1	27.5	30.9
100Li/Mg	0.4	0.5	0.5	0.5	0.8	0.6	0.5	0.4
1000Li/K	1.4	0.9	0.9	1.6	0.9	1.6	0.5	0.4

*highly erratic values are excluded from Table 6

TABLE 4—CONTINUED

Rock Type	GM-2				GM-3			GR-1
Sample No.	(9)M1–15	(10)M1–9	(11)M1–7	(12)M1–4B	(13)M1–24	(14)M1–23	(15)M1–6	(16)MD11
Trace elements (ppm)								
Li	19	15	15	18	6	6	9	50
F	474	585	538	454	623	488	508	585
Rb	527	476	441	320	475	445	644	469
Sr	81	81	123	81	86	70	64	40
Ba	371	530	495	390	495	400	442	338
Zr	93	85	109	93	103	73	77	77
Sn	7.5	15.0	12.5	12.5	3.5	5.0	10.0	2.0
W	7.6	14.4	9.2	13.3	9.0	7.9	12.2	7.6
Cu	50	127	38	50	195	207	31	N.D.
Pb	80	80	60	56	72	80	56	80
Zn	39	48	30	39	13	13	19	36
Ni	16	6	16	25	6	10	20	6
La	45	38	28	24	32	26	18	56
Ce	48	75	50	48	49	36	37	76
U	20.0	17.5	15.9	14.9	22.7	19.1	15.7	19.3
Elemental ratios								
K/Rb	87.1	95.9	103.5	110.3	98.1	107.8	70.9	85.7
Ba/Rb	0.7	1.1	1.1	1.2	1.0	0.9	0.7	0.7
K/Ba	123.7	86.2	92.2	90.5	94.1	120.0	103.3	118.9
Rb/Sr	6.5	5.9	3.6	4.0	5.5	6.4	10.1	11.7
Ca/Sr	41.5	73.2	19.87	42.4	28.3	42.9	38.0	219.8
Zr/Sn	12.4	5.7	8.7	7.4	29.4	14.6	7.7	38.5
Zn/Pb	0.5	0.6	0.5	0.7	0.2	0.2	0.3	0.5
F/Li	25.0	39.0	35.9	25.2	103.8	81.3	56.4	11.7
100Li/Mg	0.6	0.5	0.5	0.4	0.5	0.5	0.8	1.5
1000Li/K	0.4	0.3	0.3	0.5	0.1	0.1	0.2	1.22

N.D. = not detected

TABLE 4—CONTINUED

Rock Type	GR-1			GR-2		GR-3			
Sample No.	(17)MD10	(18)MD6	(19)MD7	(20)MD22	(21)MD24	(22)MD35	(23)MD16	(24)MD13	(25)MD21
Trace elements (ppm)									
Li	19	28	43	26	25	6	6	10	13
F	513	717	745	324	319	105	139	187	265
Rb	353	423	456	514	611	564	648	574	550
Sr	84	65	51	30	22	14	7	11	19
Ba	783	606	531	164	152	58	54	45	208
Zr	109	91	101	68	45	35	34	13	40
Sn	1.0	2.0	1.0	7.5	7.5	6.0	3.5	5.5	2.0
W	2.6	5.4	6.1	4.7	10.7	7.8	3.6	4.0	3.3
Cu	N.D.	N.D.	N.D.	N.D.	N.D.	N.D.	N.D.	N.D.	N.D.
Pb	68	85	85	202	72	105	80	56	60
Zn	42	39	37	35	28	13	7	14	10
Ni	20	20	16	6	16	6	10	10	N.D.
La	64	51	53	27	23	31	28	17	N.D.
Ce	103	94	92	31	48	28	42	15	23
U	13.9	8.6	20.1	20.9	23.1	20.1	9.3	3.4	22.1
Elemental ratios									
K/Rb	109.4	95.6	88.7	80.4	64.5	73.3	62.9	61.3	78.0
Ba/Rb	2.2	1.4	1.2	0.3	0.3	0.1	0.1	0.1	0.4
K/Ba	49.3	66.7	76.1	252.1	259.4	712.8	754.8	782.2	206.3
Rb/Sr	4.2	6.5	8.9	17.1	27.8	40.3	92.6	52.2	29.0
Ca/Sr	129.3	123.2	183.6	109.6	236.9	347.1	173.6	201.4	79.0
Zr/Sn	109.0	45.5	101.0	9.1	6.0	5.8	9.7	2.4	20.0
Zn/Pb	0.6	0.5	0.4	0.2	0.4	0.1	0.1	0.3	0.2
F/Li	27.0	25.6	17.3	12.5	12.8	17.5	23.2	18.7	20.4
100Li/Mg	0.3	0.6	0.9	0.9	1.2	1.7	3.3	1.8	1.7
1000Li/K	0.5	0.7	1.1	0.6	0.6	0.2	0.2	0.3	0.3

N.D. = not detected

TABLE 5

VALUES OF MAJOR ELEMENT-OXIDES (WT.%) AND DIFFERENTIATION INDEX OF THE MAE CHEDI GRANITES SHOWING RANGE, MEAN AND STANDARD DEVIATION

Rock Type	GM–1			GM–2			GM–3			GR–1			GR–2			GR–3		
No. of analyses	6			6			3			4			2			4		
	Range	$\bar{X}$	SD	Range	$\bar{X}$	SD	Range	$\bar{X}$	SD	Range	$\bar{X}$	SD	Range	$\bar{X}$	SD	Range	$\bar{X}$	SD
SiO_2	68.16–17.43	69.68	1.35	72.19–73.36	72.67	0.44	74.14–74.72	74.40	0.29	71.65–73.05	72.65	0.67	74.34–75.24	74.79	0.64	76.33–77.26	76.65	0.44
TiO_2	0.28– 0.54	0.44	0.11	0.22– 0.30	0.24	0.03	0.11– 0.15	0.13	0.02	0.24– 0.35	0.29	0.05	0.17– 0.22	0.20	0.04	0.06– 0.07	0.07	0.01
Al_2O_3	14.50–15.42	15.11	0.38	13.73–14.58	14.18	0.36	14.21–14.50	14.31	0.17	13.65–14.25	14.04	0.28	13.29–13.65	13.47	0.25	12.88–13.36	13.10	0.20
Fe_2O_3	1.03– 1.51	1.23	0.18	0.81– 1.42	1.00	0.23	0.16– 0.35	0.27	0.10	0.69– 1.06	0.88	0.16	0.92– 0.98	0.95	0.04	TR.– 0.33	0.18	0.14
FeO	0.82– 1.87	1.54	0.49	0.37– 0.72	0.53	0.13	0.08– 0.10	0.09	0.01	0.77– 1.23	0.98	0.21	0.22– 0.58	0.40	0.25	0.05– 0.12	0.10	0.03
MnO	0.04– 0.10	0.07	0.02	0.01– 0.03	0.02	0.01	N.D.	–	–	0.02– 0.04	0.03	0.01	0.03– 0.07	0.05	0.03	N.D.	–	–
MgO	0.76– 1.91	1.45	0.45	0.49– 0.86	0.61	0.13	0.19– 0.20	0.19	0.01	0.57– 1.04	0.80	0.19	0.36– 0.49	0.43	0.09	0.03– 0.13	0.08	0.04
CaO	1.09– 1.76	1.43	0.23	0.33– 0.95	0.57	0.26	0.34– 0.42	0.37	0.05	1.12– 1.52	1.30	0.17	0.46– 0.76	0.61	0.21	0.17– 0.68	0.34	0.23
Na_2O	2.69– 3.01	2.87	0.13	2.91– 3.49	3.12	0.21	2.47– 2.99	2.68	0.27	2.67– 2.96	2.84	0.12	2.79– 3.14	2.97	0.25	3.09– 3.59	3.36	0.24
K_2O	4.03– 5.03	4.51	0.45	4.25– 5.53	5.07	0.53	5.50– 5.78	5.63	0.14	4.65– 4.87	4.81	0.11	4.75– 4.98	4.87	0.16	4.24– 5.17	4.83	0.41
P_2O_5	0.11– 0.19	0.15	0.04	0.11– 0.13	0.12	0.01	0.10– 0.14	0.12	0.02	0.07– 0.11	0.09	0.02	0.05	0.05	0.00	0.01– 0.05	0.03	0.02
H_2O^+	1.21– 1.67	1.39	0.18	1.03– 1.78	1.44	0.31	1.04– 1.66	1.29	0.33	0.76– 1.34	1.00	0.26	1.14– 1.53	1.34	0.28	0.59– 1.05	0.87	0.20
D.I.	78. 5–87.0	82.6	3.3	89. 1–92.9	91.4	1.5	93. 9–94.6	94.2	0.4	85. 4–88.7	87.3	1.5	92.1	92.1	0.00	95. 1–97.0	96.0	0.8

$\bar{X}$ = mean, SD = standard deviation, D.I. = differentiation index, TR. = trace, N.D. = not detected

TABLE 6

VALUES OF TRACE ELEMENTS (PPM) OF THE MAE CHEDI GRANITES SHOWING RANGE, MEAN AND STANDARD DEVIATION

Rock Type	GM–1			GM–2			GM–3			GR–1			GR–2			GR–3		
No. of analyses	6			6			3			4			2			4		
	Range	$\bar{X}$	SD	Range	$\bar{X}$	SD	Range	$\bar{X}$	SD	Range	$\bar{X}$	SD	Range	$\bar{X}$	SD	Range	$\bar{X}$	SD
Li	34–55	45	10	15–19	17	2	6–9	7	2	19–50	35	14	25–26	26	1	6–13	9	3
F	1012–1665	1340	241	454–585	506	51	488–623	540	73	513–745	640	110	319–324	322	4	105–265	174	69
Rb	344–431	387	30	320–527	428	72	445–644	521	107	353–469	425	52	514–611	563	69	550–648	584	44
Sr	62–157	99	35	74–123	88	18	64–86	73	11	40–84	60	19	22–30	26	6	7–19	13	5
Ba	516–812	643	127	371–563	484	84	400–495	446	48	338–783	565	184	152–164	158	8	45–208	91	78
Zr	97–176	140	29	85–109	98	10	73–103	84	16	77–109	95	14	45–86	57	16	13–40	31	12
Sn	3.0–10.0	6.5	2.3	1.0–17.5	11.0	6	3.5–10.0	6.2	3.4	1.0–2.0	1.5	0.6	7.5	7.5	0	2.0–6.0	4.3	2
W	6.4–18.2	10.4	5.1	6.1–23.3	12.3	6.3	7.9–12.2	9.7	2.2	2.6–7.6	5.4	2.1	4.7–10.7	7.7	4.2	3.3–7.8	4.7	2.1
Cu	18–70	44	22	18–127	52	39	31–207	144	98	N.D.	–	–	N.D.	–	–	N.D.	–	–
Pb	50–85	67	12	56–86*	66	13	56–86	69	12	68–85	80	8	72–202	137	92	56–105	75	22
Zn	56–113*	87	22	30–48*	39	6	13–19	15	3	36–42	39	3	35–28	32	5	7–14	11	3
Ni	20–40*	29	10	6–25*	18	8	6–20	12	7	6–20	16	7	6–16	11	7	N.D.–10	7	5
La	43–69	55	11	24–58	36	13	18–32	25	7	51–64	56	6	23–27	25	3	N.D.–31	19	14
Ce	73–166	11	37	48–90	62	17	36–49	41	7	76–103	91	11	31–48	40	12	15–42	27	11
U	10.5–22.6	16.2	4.7	14.9–20.2	17.4	2.3	15.7–22.7	19.2	3.5	8.6–20.1	15.5	5	20.9–23.1	22.0	1.6	3.4–22.1	13.7	8.9

$\bar{X}$ = mean, SD = standard deviation, N.D. = not detected, *from 5 samples of analyses (see Table 4)

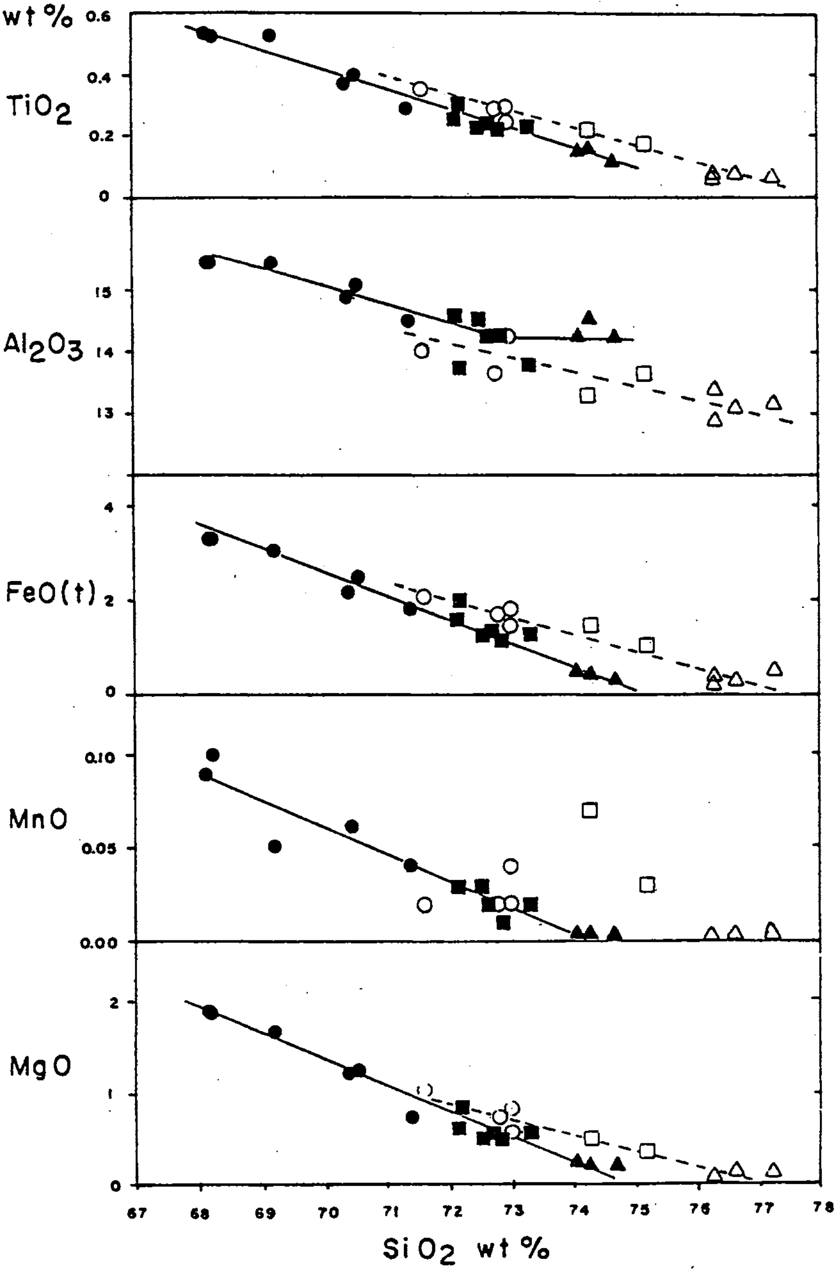

Fig. 8 Variation of major element-oxides against silica for the Mae Chedi granites.

Continued from previous page

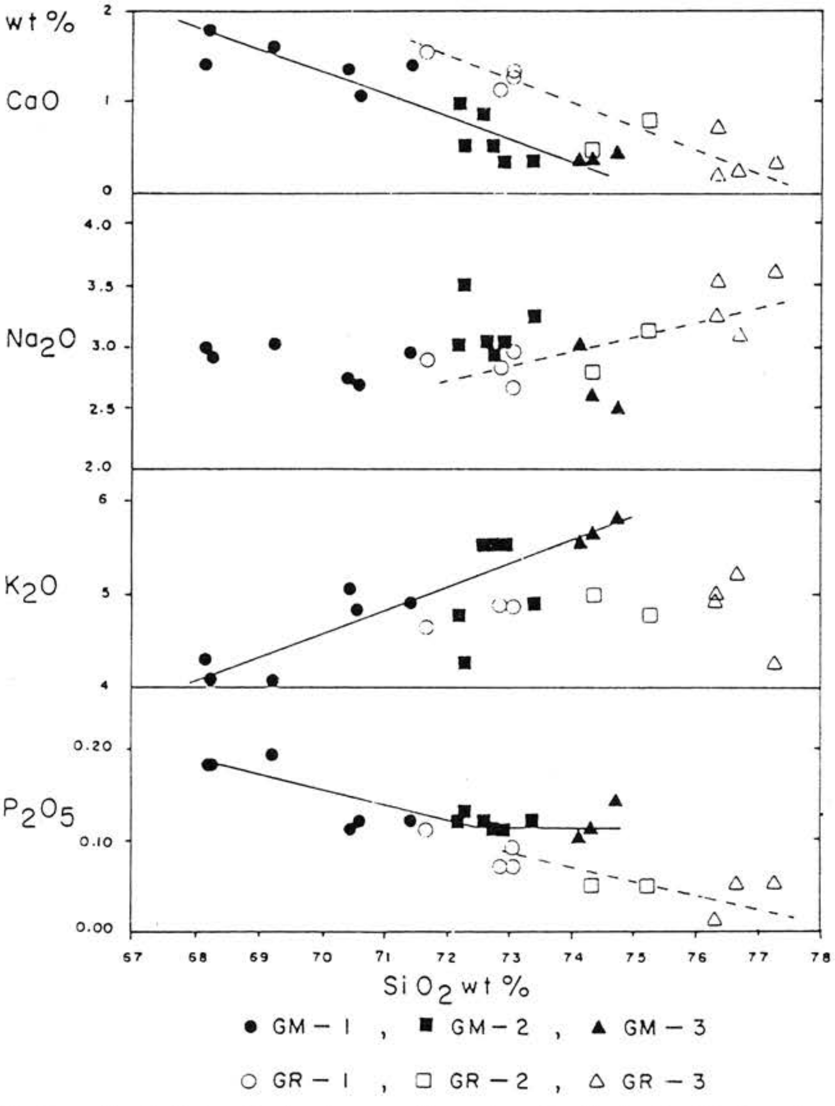

Fig. 8 cont'd. Variation of major element-oxides against silica for the Mae Chedi granites.

presents the major element-oxides together with their CIPW norms and differentiation index (D.I.) whereas Table 4 shows their trace elements and some certain elemental ratios. Range, mean and standard deviation of each of the major element-oxide together with D.I. and trace element from diverse rock types are summarized in Table 5 and 6 respectively. The differentiation index is computed as the sum of normative quartz, orthoclase and albite which recalculated after the total normative composition are normalized to 100 percent (Thornton and Tuttle, 1960).

Major element-oxide variations

Variations diagrams of the major element-oxides plot against silica (Figure 8) illustrates that there are two distinct trends. The first trend (GM-series) is composed of the GM-1, the GM-2, and GM-3. The second trend (GR-series) consists of the GR-1,

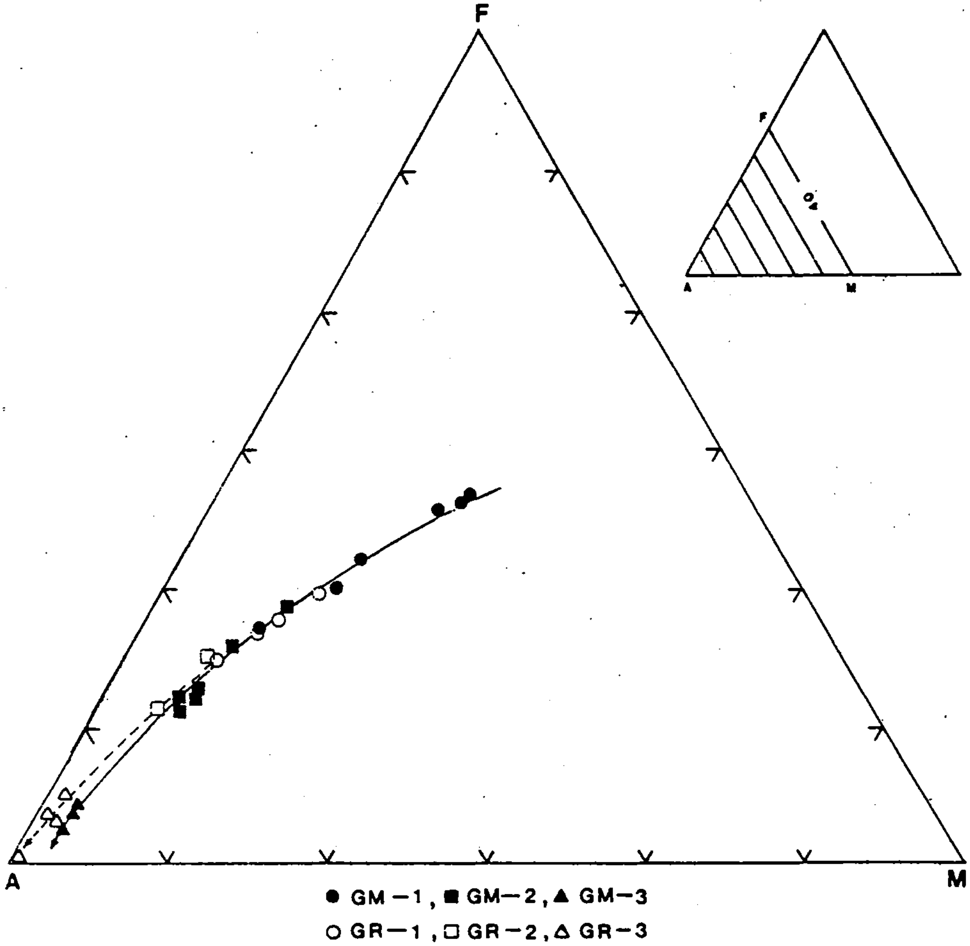

Fig. 9. A ($Na_2O + K_2O$) – M (MgO) diagram for the Mae Chedi granites showing chemical variation trends.

the GR-2, and the GR-3. It is noticeable that there are some differences of the same major element-oxides between these two series. The GM-series is relatively higher TiO_2, Al_2O_3, FeO (total), MnO, MgO, CaO, P_2O_5, H_2O^+ but lower SiO_2, contents than that of the GR-series. The Na_2O and K_2O contents in the GM-1, GM-2, and the GR-1, GR-2 show no significant dissimilarity. However, the GM-3 is distinctly lower in Na_2O and higher in K_2O than the GR-3. Both GM- and GR- series show increasing contents of K_2O and Na_2O and decreasing contents of TiO_2, Al_2O_3, FeO(total), MnO, MgO, CaO, and P_2O_5 as SiO_2 content increases.

The AFM diagram shows another well-defined variation of the GM- and the GR-series (Figure 9). Both variation trends are close to the F-A join and move toward the A apex. The decreasing total iron as well as MgO and enrichment of total alkalis are characteristic of both trends. The K_2O-Na_2O-CaO diagram also shows increasing alkalis for both series (Figure 10). However, the trend of the GM-series has a tendency

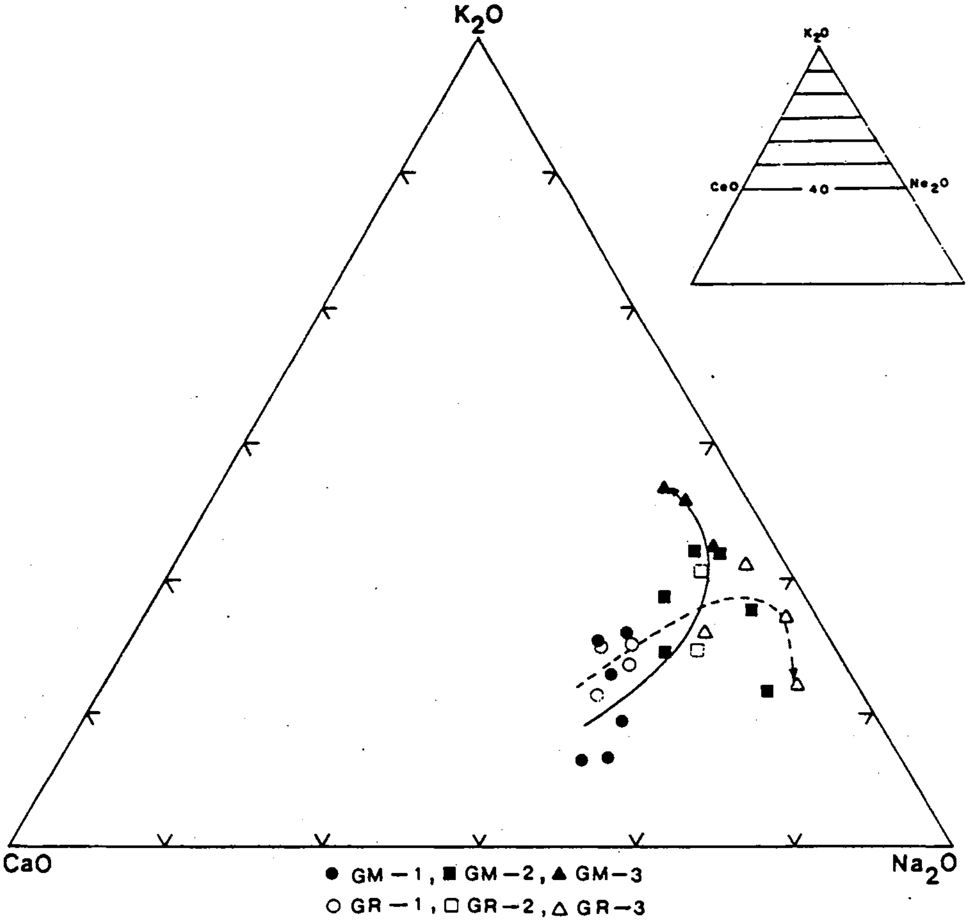

Fig. 10. K_2O – Na_2O – CaO diagram for the Mae Chedi granites showing chemical variation trends.

Continued from previous page

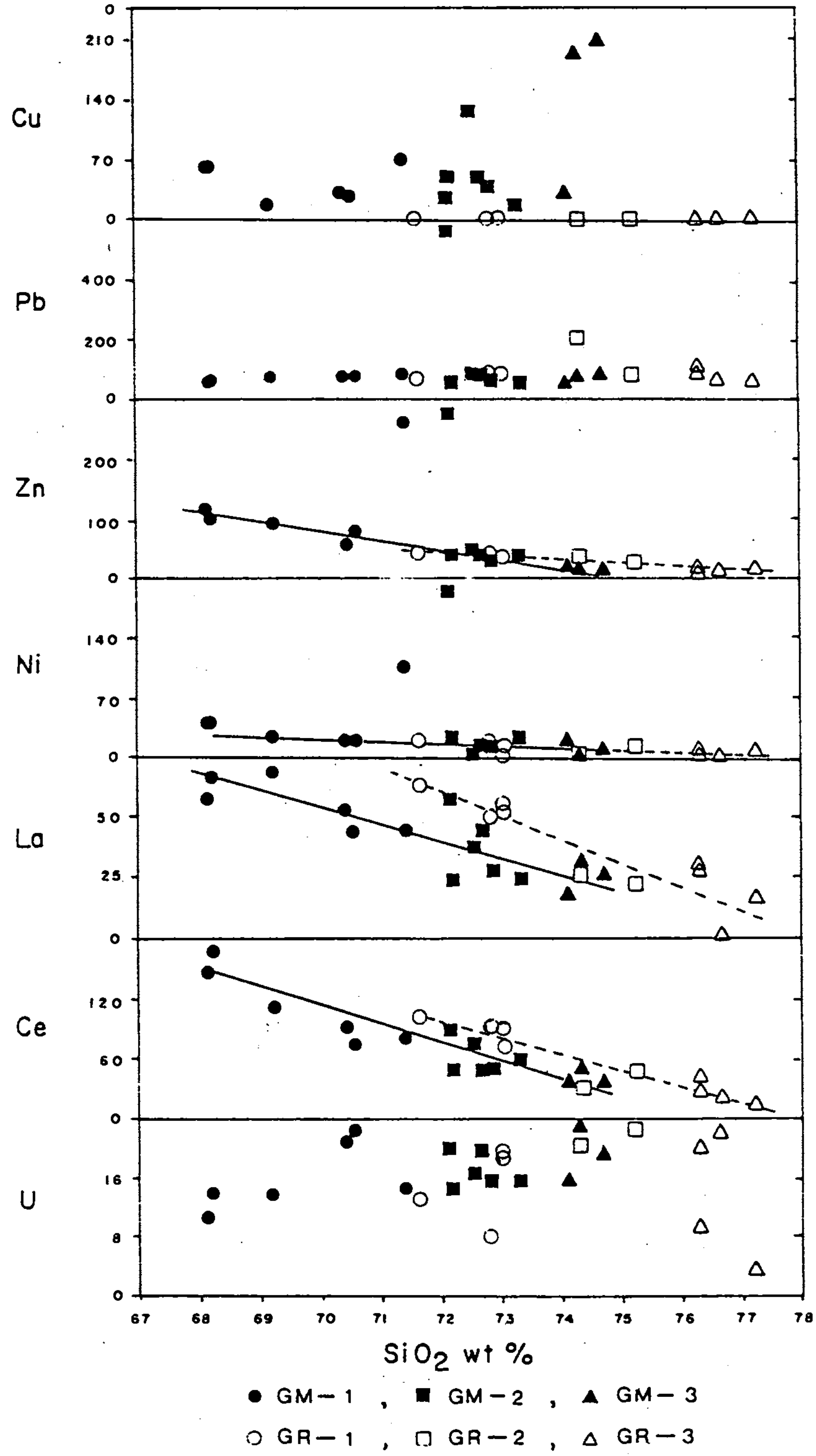

Fig. 12 cont'd. Variation of trace elements against silica for the Mae Chedi granites.

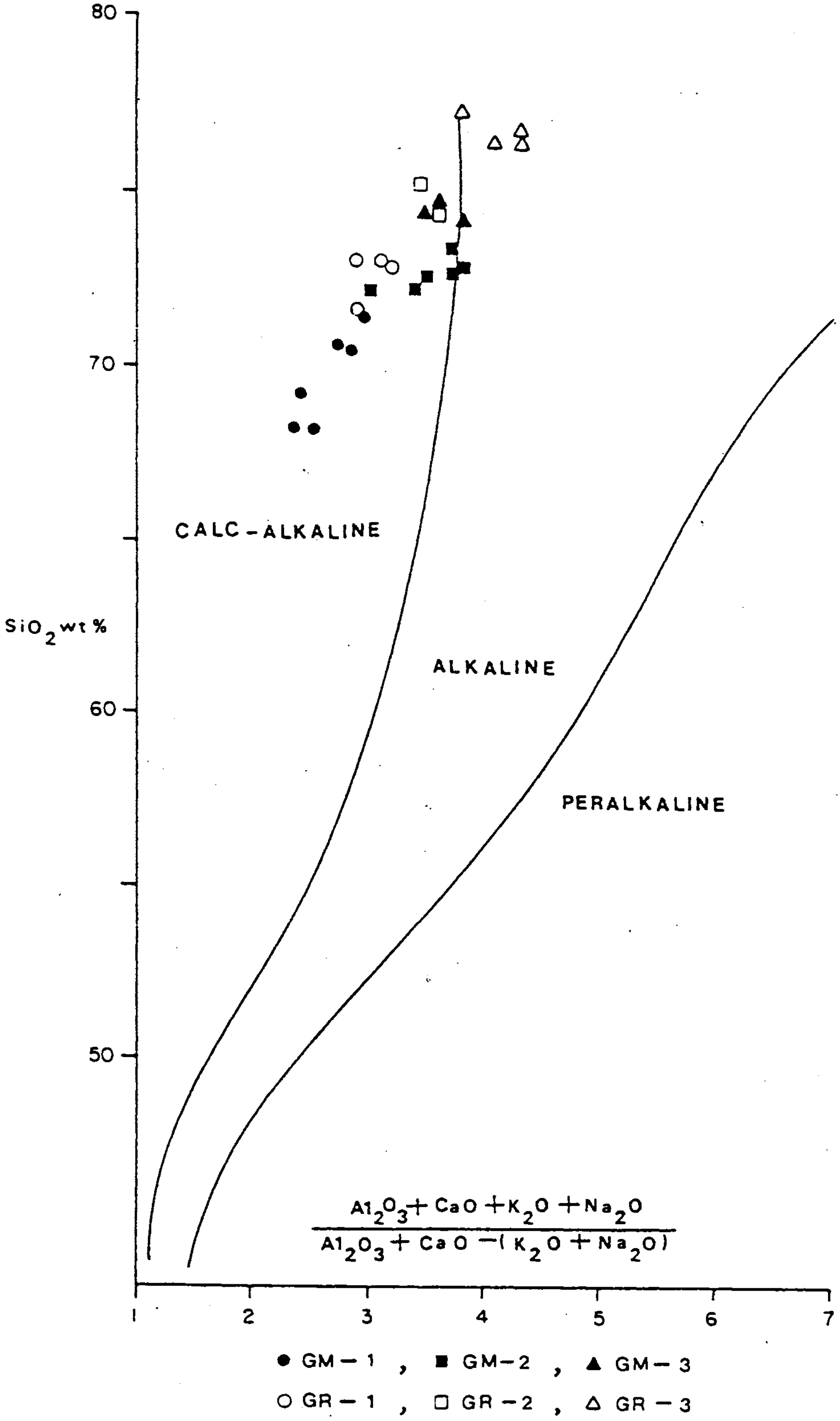

Fig. 11. Alkalinity ratio variation diagram for the Mae Chedi granites. The alkalinity fields are from Wright (1969, cited in Sheraton and Labonne, 1978).

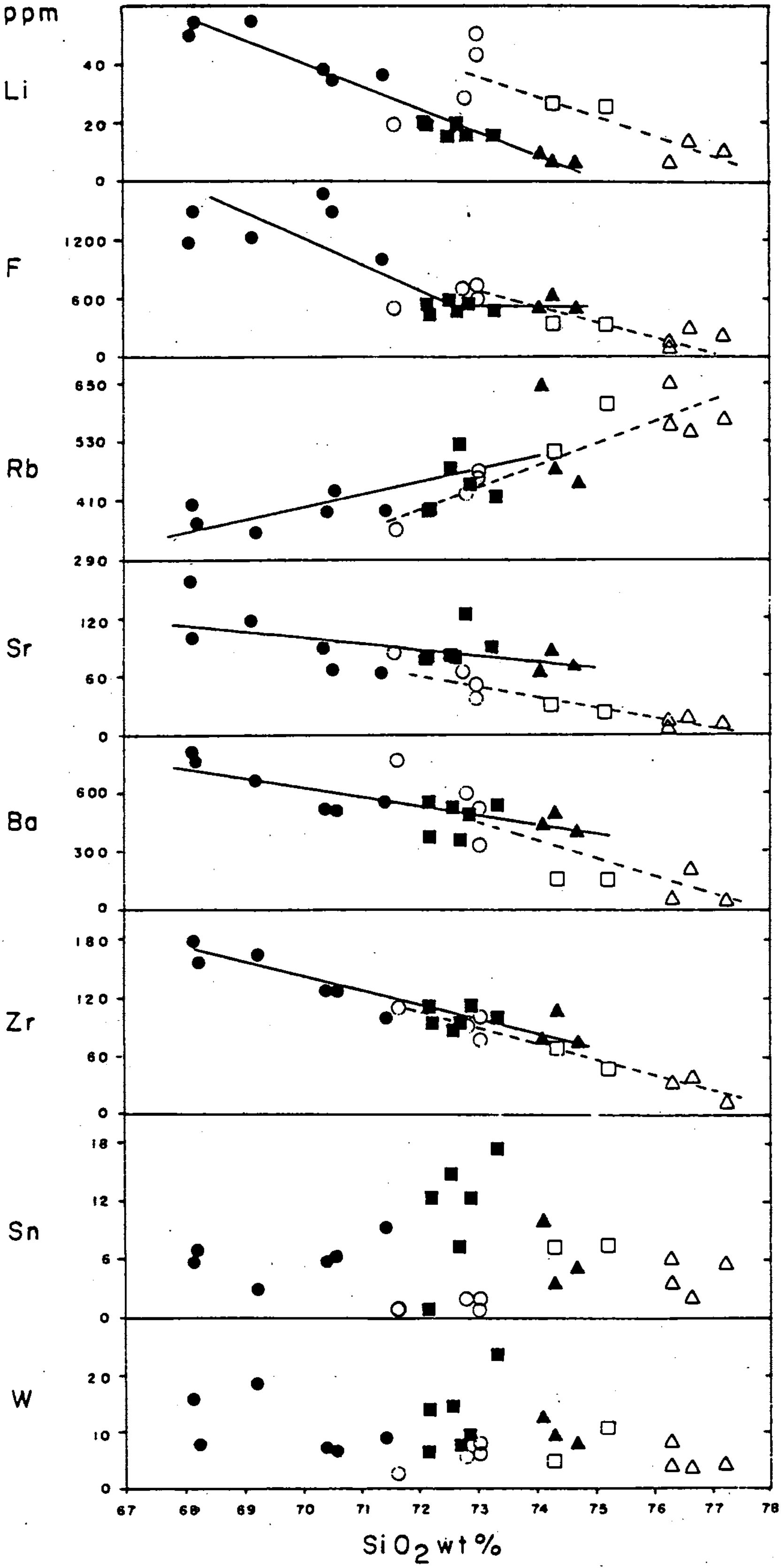

Fig. 12 Variation of trace elements against silica for the Mae Chedi granites.

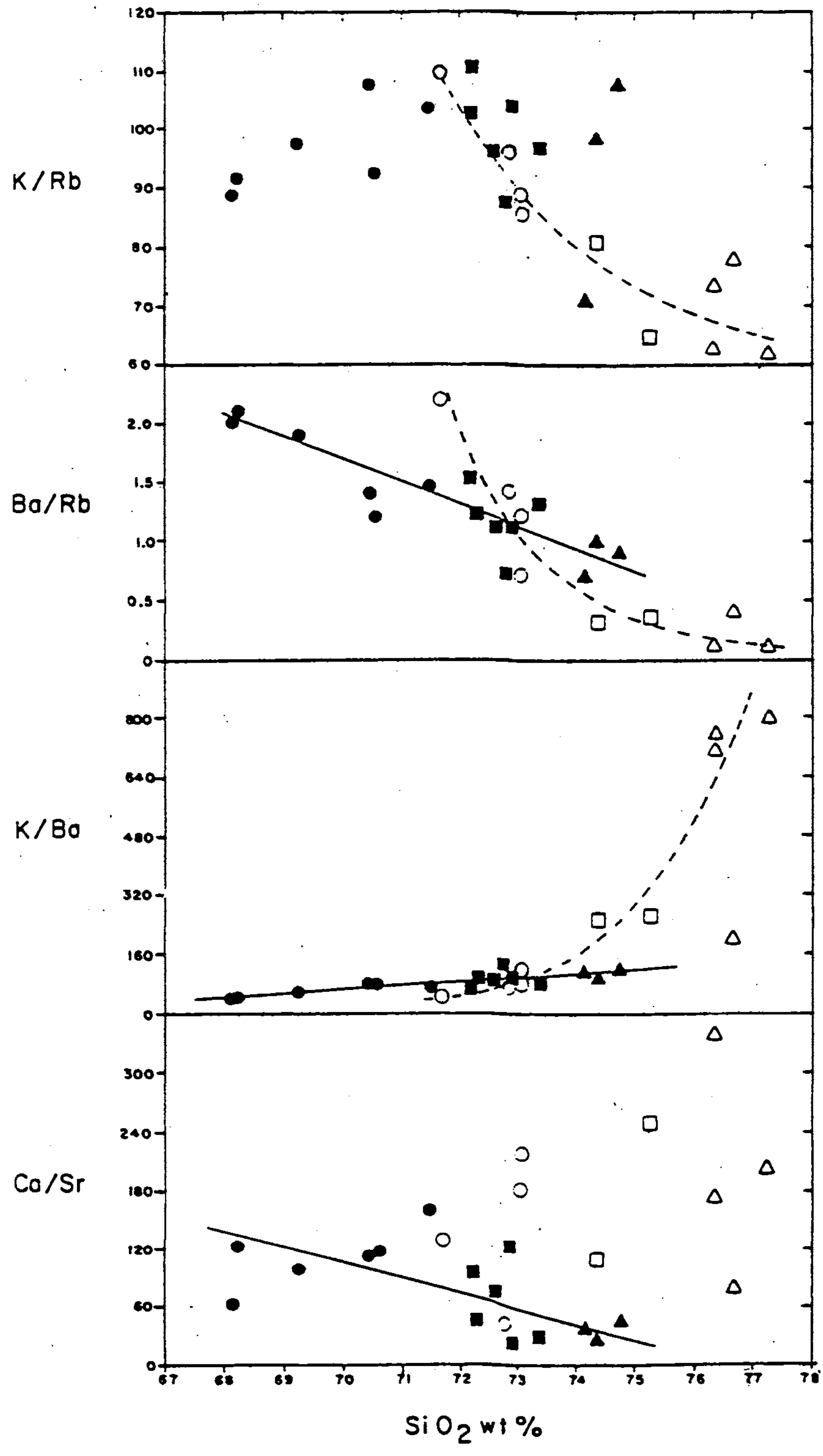

Fig. 13 Variation of the K/Rb, Ba/Rb, K/Ba, Ca/Sr, Rb/Sr, F/Li and 100 Li/Mg ratios against SiO_2 for the Mae Chedi granites.

Continued from previous page

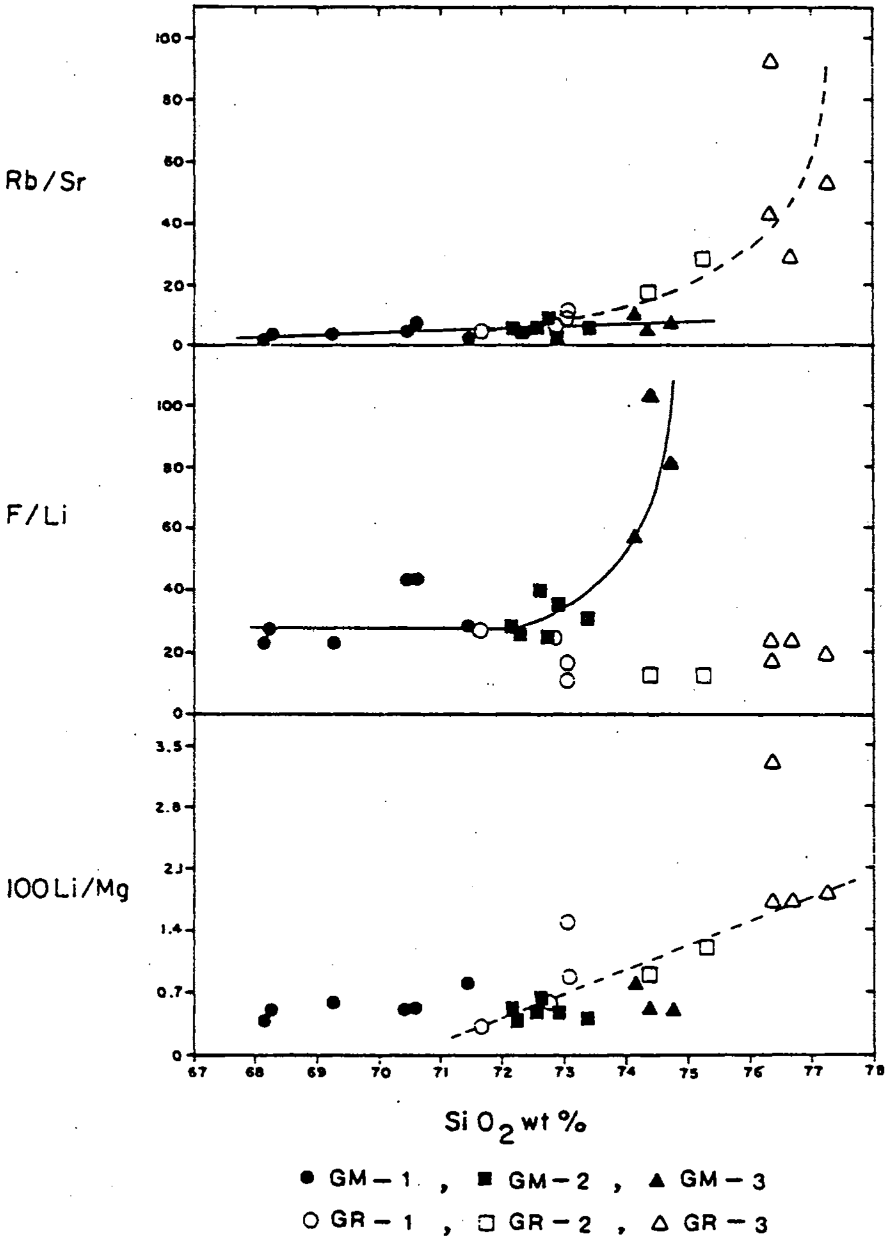

Fig. 13 cont'd. Variation of the K/Rb, Ba/Rb, K/Ba, Ca/Sr, Rb/Sr, F/Li and 100 Li/Mg ratios against SiO_2 for the Mae Chedi granites.

to move toward the K_2O whereas the trend of the GR-series has a tendency to move toward the Na_2O. The plotting of the alkainity ratio proposed by Wright (1969, cited in Sheraton and Labonne, 1978) against SiO_2 shows that majority of samples of the GM- and the GR-series fall in the calc-alkaline field, although some of the high silicic samples, especially the GR-3, fall in the alkaline field (Figure 11).

Trace element variations

Most of the variations constructed from plots of the trace elements (Table 4) against SiO_2, again, tend to show two distinct trends of the GM- and the GR-series (Figure 12). There are also some differences of the same trace element between the GM- and the GR-series, the former is notably higher in Li, F, Sr, Ba, Zr, Sn, W, Cu, Zn, Ni, Ce, and lower in Rb contents than the latter. No significant differences of Pb, La, and U is known from these two granitic series.

Some selected elemental ratios (K/Rb, Ba/Rb, K/Ba, Ca/Sr, Rb/Sr, F/Li, 100 Li/Mg) plotted against SiO_2 content are shown in Figure 13. The K/Rb and Ba/Rb ratios of the GR-series distinctively decrease from the GR-1 to the GR-3 whereas the K/Rb ratios of the GM-series seem to be scattered and show just slight increase, but the Ba/Rb ratios appear to decrease gradually from the GM-1 to the GM-3 with increasing SiO_2. The concentration of the K/Ba, Rb/Sr and 100 Li/Mg ratios of the GR-series distinctly increase from the GR-1 to the GR-3 while the K/Ba and the Rb/Sr ratios of the GM-series slightly increase from the GM-1 to the GM-3 with an increase of SiO_2, but the 100 Li/Mg ratios of the GM-series do not change. The Ca/Sr ratios of the GM-series decrease from the GM-1 to the GM-3 while those of the GR- series seem to be scattered. The average values of Ca/Sr ratio of the GR-series in Table 4 appear to increase from the GR-1 to the GR-3 as the silica content increases. It should be noted

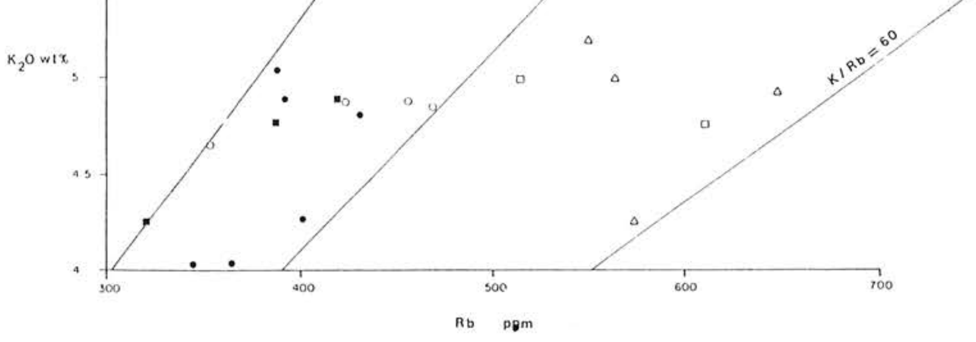

Fig. 14 Plots of K_2O, Sr, and Ba contents against Rb content for the Mae Chedi granites.

Continued from previous page

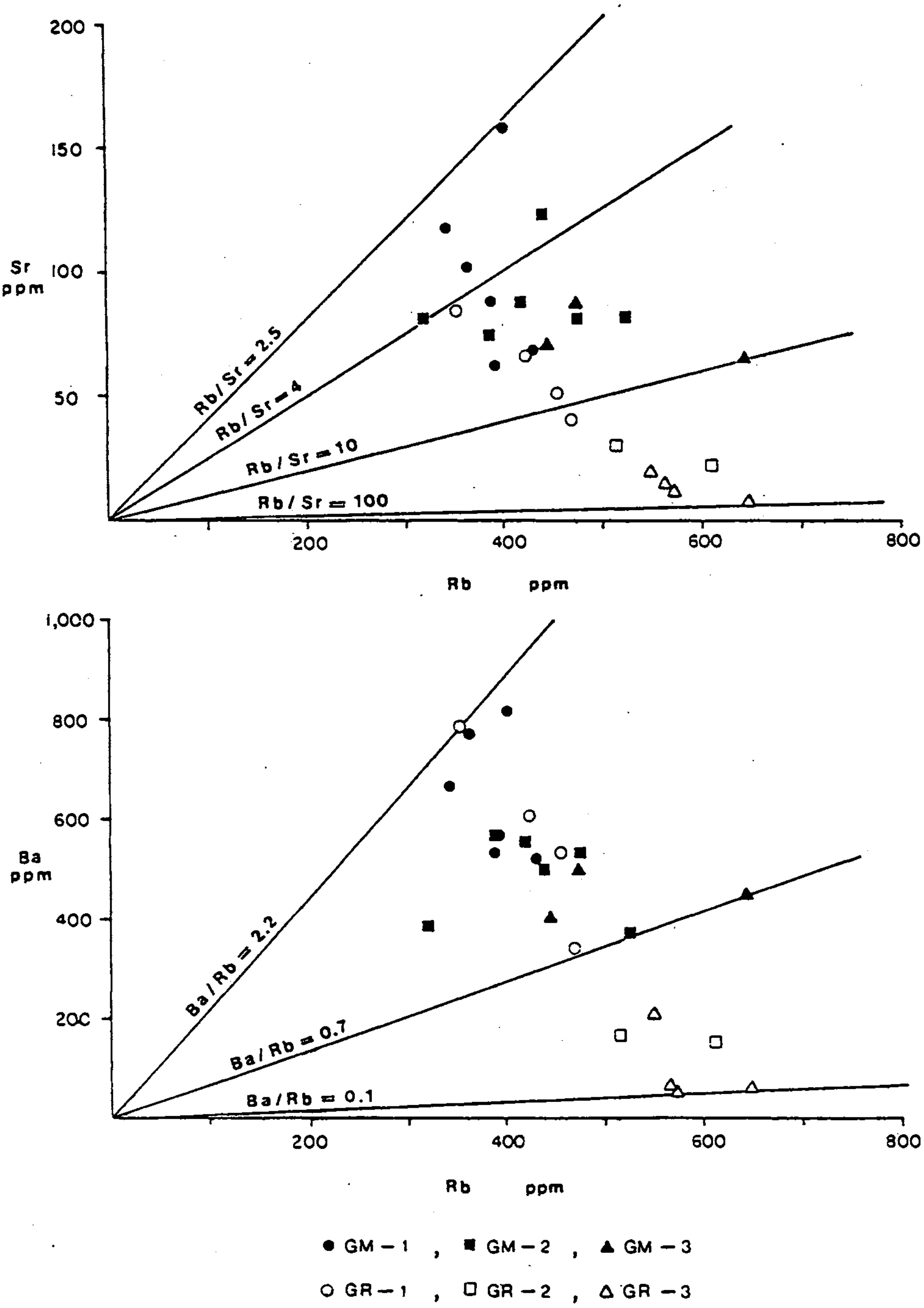

Fig. 14 cont'd. Plots of K_2O, Sr, and Ba contents against Rb content for the Mae Chedi granites.

that the F/Li ratios of the GM-series appear to be unchanged from the GM-1 to the GM-2 but abruptly increase from the GM-2 to the GM-3 while those of the F/Li ratios of GR-series show no significant trend.

Plots of the K_2O, Sr, and Ba contents against the Rb content (Figure 14) show that the GM-3 has higher K/Rb and Ba/Rb and lower Rb/Sr ratios than the GR-3. It is important to note that the K/Rb, Ba/Rb, and Rb/Sr ratios of the GM-series are relatively restricted, i.e. ranging from 70.9 to 110.3 (87.1 to 110.3, except for the sample (15) M1–6), 0.7 to 2.1 and 2.6 to 10.1 whereas those fo the GR-series are relatively wider ranges, i.e. varying from 61.3 to 109.4, 0.1 to 2.2 and 4.2 to 92.6, respectively (see Table 4).

Metabasites

The chemical analyses and CIPW norm together with differentiation index (Thornton and Turtle, 1960) of a total of 7 samples of metabasites from the Mae Chedi area are given in Table 7 and 8 respectively. The location of analysed metabasite specimens are shown in Figures 3, 4. Plots of the $Na_2O + K_2O$ against the SiO_2 on the diagram for nomenclature and classification of volcanic rocks (after Cox *et al.*, 1979) in Figure 15, reveal that all of the originally volcanic rocks which had been

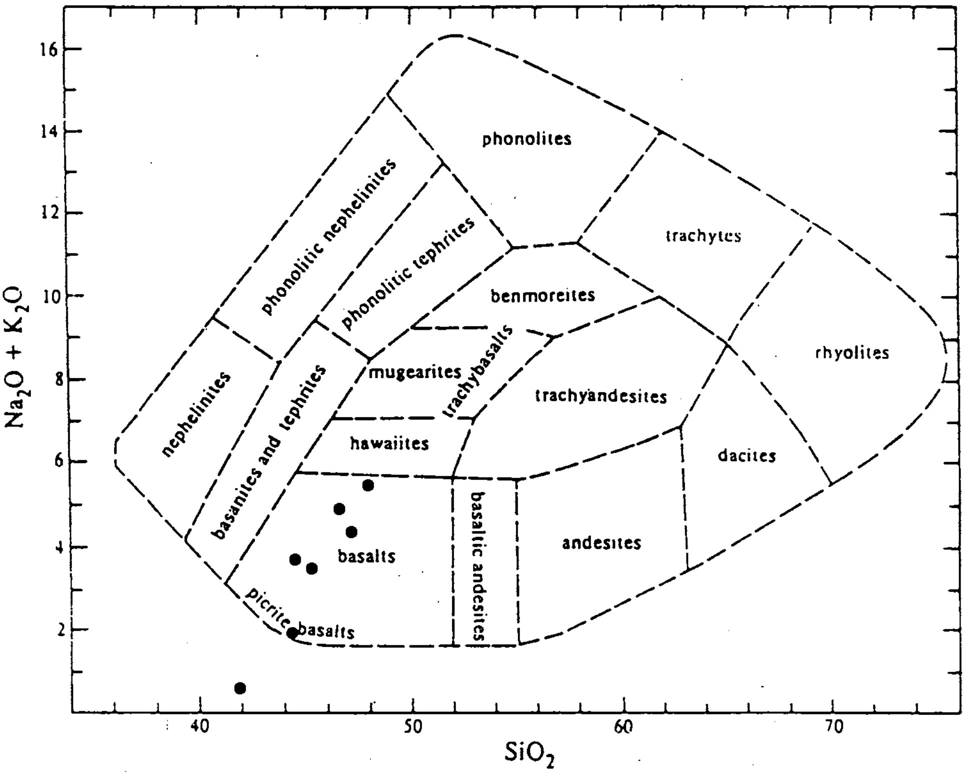

Fig. 15. Plots of $Na_2O + K_2O$ against SiO_2 for metabasites of the Mae Chedi. Nomenclature and boundaries of volcanic rocks are from Cox *et al.* (1979).

TABLE 7

CHEMICAL ANALYSES OF METABASITES, MAE CHEDI, WIANG PA PAO, CHIANG RAI

Sample No.	B1 (M1-5)	B2 (V1-1)	B3 (V1-2)	B4 (M2-1)	B5 (M2-2)	B6 (MD31)	B7 (MD26)
Grid Ref.	499142	499141	499141	501138	501138	496159	479186
Major elements (wt.%)							
SiO_2	45.21	47.90	44.37	46.90	44.57	46.46	41.79
TiO_2	3.04	2.43	2.53	2.46	2.72	3.16	2.46
Al_2O_3	16.67	16.93	11.59	16.31	16.67	16.67	10.99
Fe_2O_3	2.99	2.57	2.33	2.52	2.62	2.95	2.01
FeO	8.56	6.69	9.71	8.15	9.07	8.77	9.62
MnO	0.20	0.35	0.27	0.15	0.20	0.15	0.13
MgO	7.05	6.68	14.05	6.49	6.69	5.26	18.70
CaO	9.80	8.35	10.85	10.90	11.30	9.20	9.05
Na_2O	2.53	3.16	1.21	2.61	2.27	3.22	0.45
K_2O	1.00	2.31	0.71	1.74	1.40	1.71	0.15
P_2O_5	0.51	0.34	0.34	0.37	0.37	0.51	0.31
S	0.97	0.05	0.11	0.18	0.30	0.51	N.D.
H_2O^+	1.04	1.67	1.26	1.06	1.11	1.21	3.78
Total	99.57	99.43	99.33	99.84	99.29	99.78	99.44
Trace elements (ppm)							
Li	18	26	21	39	40	35	6
F	1611	3276	3774	1355	1974	1124	510
Sn	2.5	<1	1.5	2.5	1.5	<1	<1
W	6.9	2.9	1.8	3.7	1.5	2.9	0.9
Cu	456	71	50	185	29	50	93
Pb	35	50	50	35	35	35	30
Zn	122	126	127	113	129	126	124
Ni	100	80	650	70	100	50	900
U	2.0	1.2	1.1	1.1	0.9	1.7	1.3

N.D. = not detected

TABLE 8

CIPW NORMS AND DIFFERENTIATION INDEX (D.I.) OF METABASITES, MAE CHEDI, WIANG PA PAO, CHIANG RAI

Sample No.	B1 (M1–5)	B2 (V1–1)	B3 (V1–2)	B4 (M2–1)	B5 (M2–2)	B6 (MD31)	B7 (MD26)
Or	5.91	13.65	4.20	10.28	8.27	10.10	0.89
ab	21.41	24.03	10.24	18.84	14.97	25.07	3.81
an	31.17	25.19	24.10	27.65	31.16	25.98	27.53
ne	–	1.47	–	1.76	2.30	1.18	–
di wo	5.90	5.85	11.49	10.02	9.39	6.82	6.41
di en	3.96	3.87	7.87	6.14	5.61	4.08	4.62
di fs	1.49	1.56	2.70	3.32	3.29	2.39	1.21
hy en	4.86	–	5.54	–	–	–	14.01
hy fs	1.83	–	1.90	–	–	–	3.67
Ol fo	6.13	8.95	15.12	7.02	7.74	6.32	19.58
Ol fa	2.54	3.97	5.72	4.18	5.00	4.09	5.65
Ol fa	2.54	3.97	5.72	4.18	5.00	4.09	5.65
Ol fa	2.54	3.97	5.72	4.18	5.00	4.09	5.65
mt	4.33	3.73	3.38	3.65	3.80	4.28	2.92
il	5.77	4.61	4.81	4.67	5.17	6.00	4.67
pr	1.82	0.09	0.21	0.34	0.56	0.96	–
ap	1.18	0.79	0.79	0.86	0.86	1.18	0.72
Salic tot.	58.49	64.34	38.54	58.53	56.70	62.33	32.23
Femic tot.	39.81	33.42	59.53	40.20	41.42	36.12	63.46
D.I.	27.8	40.0	14.7	31.3	26.0	36.9	4.9

metamorphosed in the Mae Chedi fall in the basaltic field, except for sample B 7 which may possibly be an ultramafic variety.

Based on the petrological and chemical data of the rocks, it is obvious that the rocks were originally basaltic in composition. Thus, the authors favour to term these rocks as "metabasites".

DISCUSSION

S-Type and I-Type Granites

Chappell and White (1974) suggested, on the basis of field evidences, petrological and geochemical data, that various granitic rocks in the southeastern Australia might have been derived from either sedimentary source rocks (S-type granites) or from igneous source rocks (I-type granites). The principal characteristics of the two contrasting granite types are summarized in Table 9.

Ishihara (1979) classified the granitoids into 2 series; the magnetite-series granitoids contain an easily recognizable amount of magnetite under the microscope, whereas the ilmenite-series rocks are practically free of opaque oxide minerals (less than 0.1 vol. %), in which ilmenite is consistently seen. Ishihara (1980) also pointed out

TABLE 9

PRINCIPAL CHARACTERISTICS OF S- AND I-TYPE GRANITES
(Modified after Chappell and White, 1974; Hine *et al.*, 1978)

S-types	I-types
(1) Relatively low sodium, Na_2O normally <3.2% in rocks with approx. 5% K_2O, decreasing to <2.2% in rocks with approx. 2% K_2O	(1) Relatively high sodium, Na_2O normally >3.2% in felsic varieties decreasing to >2.2% in more mafic types
(2) Mol. $Al_2O_3/(Na_2O+K_2O+CaO) > 1.1$	(2) Mol. $Al_2O_3/(Na_2O+K_2O+CaO) < 1.1$
(3) > 1% CIPW normative corundum	(3) CIPW normative diopside or < 1% CIPW normative corundum
(4) Relatively restricted in composition to high SiO_2 types	(4) Broad spectrum of compositions from felsic to mafic
(5) Variation diagrams irregular	(5) Regular inter-element variations within plutons; linear or near linear variation diagrams
(6) High initial $^{87}Sr/^{86}Sr$ ratios (> 0.708)	(6) Low initial $^{87}Sr/^{86}Sr$ ratios (< 0.708)
(7) Biotite abundant in more mafic types, up to 35%, and muscovite is common in more felsic types	(7) Hornblende is common in more mafic types and generally present in felsic types.
(8) Common accessory minerals include monazite, ilmenite and alumino-silicates such as garnet and cordierite, etc.	(8) Usually contain primary sphene, allanite and magnetite
(9) Hornblende-bearing xenoliths are rare but metasedimentary xenoliths are not uncommon	(9) Mafic hornblende bearing xenoliths of igneous appearance are common

that tin deposits are associated almost exclusively with ilmenite-series whereas tungsten deposits can be associated with both ilmenite and magnetite-series.

The initial $^{87}Sr/^{86}Sr$ ratio data of the porphyritic biotite granites of the Khuntan Mountain Range (see Figure 2) reported by Teggin (1975), Braun *et al.* (1976), Beckinsale (1979), and Nakapadungrat (1982) reveal that all Triassic granites are the S-type with a very high initial $^{87}Sr/^{86}Sr$ ratio ranging from 0.7244 ± 0.0020 to 0.7295 ± 0.0007. Thus, it is reasonable to believe that the porphyritic biotite granites of the Mae Chedi (GR-1), which is a part of the Khuntan Mountain Range, is the S-type and possesses the same range of $^{87}Sr/^{86}Sr$ initial ratio.

The chemical data of the Mae Chedi granites are summarized in accordance with the chemical criteria proposed by Chappell and White (1974) and shown in Table 10. Although there is the absence of actual initial $^{87}SR/^{86}Sr$ value, the data in Table 10 strongly suggest that all of the analyzed granites are peraluminous and can be classified as the S-type granites, only the GR-3 has an average Na_2O content higher (3.36%) than 3.2%. It can, therefore, be concluded that tin and tungsten deposits of the Mae Chedi Mine are possibly associated with the S-type granites. A similar suggestion of Plimer (1980) that the tin and tungsten deposits in many places, e.g. Cornwall, U.K.; Erzgebirge district, East Germany and Czechsolvakia; and the Wolfram Camp, Herberton and New England districts of Australia, are associated with the S-type granites though Chappell and White (1974) suggested that tin is associated with the S-type granites whereas tungsten and porphyry-type copper and molybdenum deposits are associated with the I-types. In their previous study in the Mae Chedi Mine (Khun Plin Mine), Suensilpong and Jungysusuk (1981) have also come to the same conclusion that tin and tungsten are associated with the S- and the I-type granites, respectively. However, the result of the present study indicates that tin as well as tungsten are conclusively associated with the S-type granites.

Table 10

GEOCHEMICAL CRITERIA OF CHAPPELL AND WHITE (1974) APPLIED TO THE MAE CHEDI GRANITES.

Rock Types	No. of Samples	Na_2O%	K_2O%	$(Na_2O + K_2O + CaO)$	Mol.Al_2O_3/ Norm C (%)
GM-1	6	2.87	4.51	1.24	3.29
GM-2	6	3.12	5.07	1.22	2.81
GM-3	3	2.68	5.63	1.28	3.41
GR-1	4	2.84	4.81	1.15	2.02
GR-2	2	2.97	4.87	1.20	2.34
GR-3	4	3.36	4.83	1.15	1.81

CIPW Norms and Their Plots in the System Quartz-Albite-Orthoclase-H_2O

CIPW norms of the Mae Chedi granites are calculated and shown in Table 3. Normative quartz, albite, and orthoclase are plotted on the experimentally derived phase diagrams in the systems Q-Ab-Or-H_2O (after Tuttle and Bowen, 1958) as shown in Figure 16. It is obvious that the sample plots of the GR-series tend to cluster on the quartz-feldspar field boundaries at 500 and 2000 bars (about 1000 bars) which is indicative of higher water pressure. Both of them seem to be in a relatively restricted composition field in the system. However the fine- to medium-grained leucocratic granite GM-3 generally contains higher normative orthoclase, instead of albite, than the fine-grained biotite granite (GM-1) which indicates that the process of K-feldspathization might have taken place late during magmatic crystallization.

The K/Rb ratios have long been suggested as a useful guide for the understanding of magmatic differentiation. Since the variation in the K/Rb ratio can be used to distinguish different types of granites which have similar mineralogy and major element contents, it

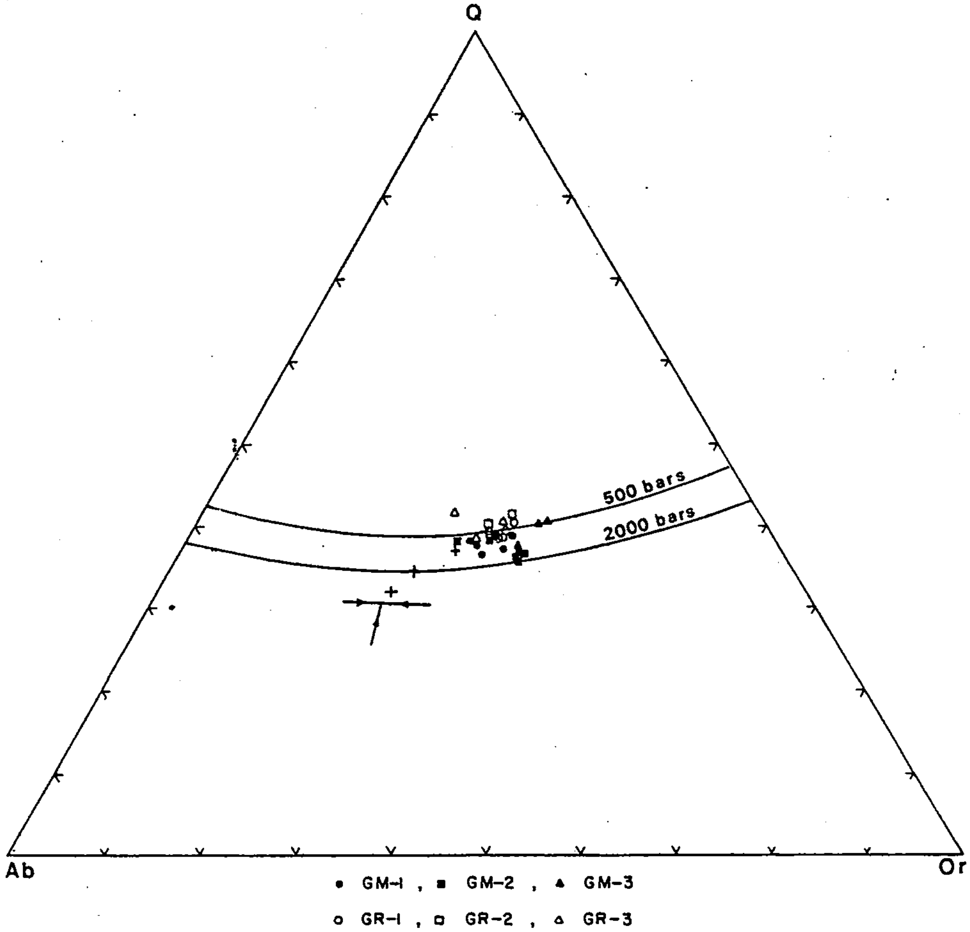

Fig. 16. Normative Q-Ab-Or diagram for the Mae Chedi granites. The quartz-feldspar field boundaries at 500 and 2000 bars P_{H_2O}, and positions of Quaternary isobaric minima are from Tuttle and Bowen (1958).

can also be used to delineate the sequence of igneous intrusion (Taylor, 1965). Taylor (*op. cit.*) also mentioned that, for a single fractionation sequence, the K/Rb ratio is likely to decrease toward the acid end of the sequence. Based on the consideration of the K/Rb as well as the Ba/Rb ratios and SiO_2 content of the GM- and the GR-series (Figure 13), it is suggested that the parent magma of the GR-series has fractionated from the GR-1 to the GR-2 and finally to the GR-3 in accordance with the decrease of both the K/Rb and the Ba/Rb ratios. These patterns are in general agreement with those studied by Taylor (*op. cit.*), Tauson and Kozlov (1973), Charusiri (1980), Charusiri and Pongsapich (1982), and Nakapadungrat (1982). In addition, the Li/Mg ratios are also useful from the differentiation point of view. For the GR-granitic series, despite the decrease in lithium content from the GR-1 to the GR-3, magnesium content also decreases at a higher order of magnitude (Figures 8, 12). As a consequence, the Li/Mg ratio of the GR-series still increases as the differentiation progresses. This is also similar to the differentiation of the Samoeng granites (Punyaprasiddihi, 1980). In contrast to the GR-series, the GM-series does not follow the differentiation trends as that observed to the GR-series. The GM-series has higher K/Rb, Ba/Rb, and F/Li and lower K/Ba, Ca/Sr, Rb/Sr, and Li/Mg ratios than that of the GR-series (as shown in Figures 13, 14) suggesting that the variations of these elemental ratios of the GM-series may have resulted from the hydrothermal alteration process instead of a differentiation process.

The trace contents of Rb, Sr, and Ba are particularly useful for modelling the granitic systems since they occur only in the major silicate minerals but not in the accessory components (McCarthy and Hasty, 1976). The change in composition of liquid phase resulting from fractional crystallization of the solid phases may be calculated by the Rayleigh fractionation law, applied by Neuman *et al.* (1954) and Greenland (1970), as in the following equations:

$$\frac{C_L}{C_O} = F^{(D_1 - 1)}$$

$$F = \frac{100-\text{percentage of crystallization}}{100}$$

where C_L is the concentration of a trace element in the liquid after removal of the crystal, C_O the original concentration of that element in the liquid, D_1 the partition or distribution coefficient (crystal/ liquid), and F the fraction of remaining liquid. Based on the above equations and partition coefficients tabulated in Table 11, the results obtained in model calculations of perfect fractional crystallization are illustrated in Figure 17.

The Rb-Sr, Rb-Ba, and Ba-Sr data plots of the Mae Chedi granites (Figure 17) clearly show that the GR-series have developed a well-defined differentiation trend starting from the GR-1 to the GR-2, and finally to the GR-3, parallel to the vector of alkali feldspar. It shows that the Rb, Sr, and Ba contents may have been influenced by crystal fractionation of alkali feldspar rather than plagioclase and biotite. On the contrary, these plots of the GM-series exhibit a cluster appearance. In terms of these distribution patterns, it is suggested that the variations of the GR-granitic series could

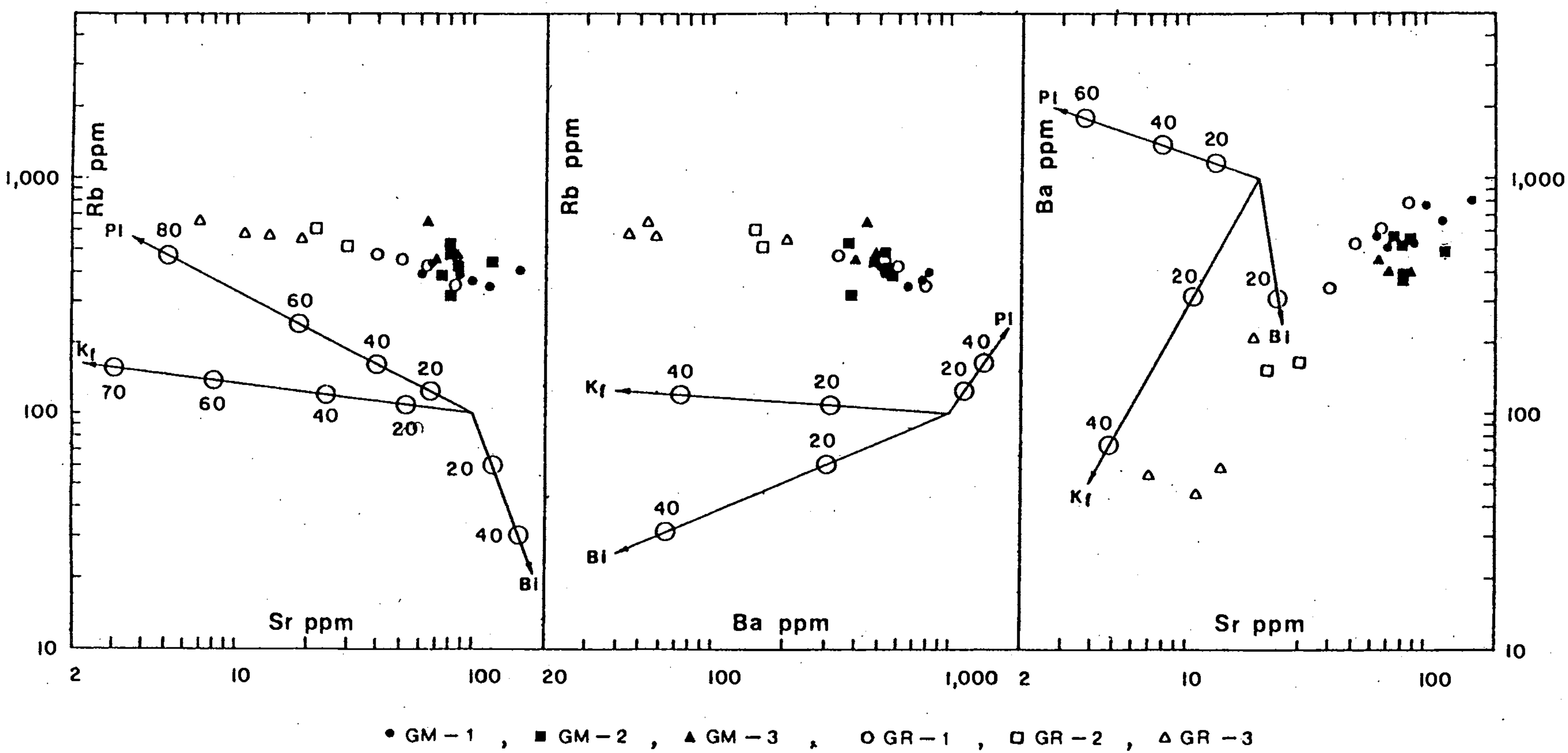

Fig. 17. Interelement correlations of Rb, Sr, and Ba for the Mae Chedi granites. The mineral vectors indicate the change in composition of liquid phases as a result of fractional crystallization of the solid phases plagioclase (Pl), alkali feldspar (K_f), and biotite (Bi), calculated by the Raleigh fractionation law, applied by Neuman *et al.* (1954) and Greenland (1970), using the distribution coefficients from Table 11. Numbers marked on the mineral vectors show the percentages of crystallization.

Table 11

PARTITION COEFFICIENTS (CRYSTAL/LIQUID) USED IN THIS STUDY.

Element	Alkali feldspar	Plagioclase	Biotite
Rb	0.659[a]	0.048[a,b]	3.26[a,b]
Sr	3.870[a]	2.804[a,b]	0.12[a,b]
Ba	6.120[a]	0.360[a,b]	6.36[a,b]

Source: a. Schnetzler and Philpotts (1970), b. Philpotts and Schnetzler (1970).

be the result of fractional crystallization and the GR-3 type represents the crystallization of the ultimate granitic residual liquid of the series. In contrast, those of the variations of the GM-granitic series could be the result of metasomatic alteration and the GM-3 represents the ultimate metasomatic alteration product of the series.

Judging from the petrology and chemistry of the granitic rocks, it has clearly been seen that the GM-series are unlikely to be related to the GR-series. Owing to the lack of the field relationship and the radiometric dating of both granitic series, the age relationship of these two granitic suites is still uncertain. However, Suensilpong and Jungyusuk (1981) suggested that fine-grained biotite granites of the Mae Chedi Mine (including Samoeng and Doi Mok Mines) are younger than porphyritic biotite granite of Upper Triassic age.

Genetic Model of Tin-Tungsten Mineralizations

Although the primary tin-tungsten mineralizations occur in the Mae Chedi area where small granitic plutons of the GM-series intruded metabasites (Figure 3), on the basis of the very low tin and tungsten contents of the metabasites (Table 7), it is reasonable to believe that the metabasites are not genetically associated with the tin-tungsten mineralizations, but they may act as a cap-rock. Furthermore, based on the field evidence and detailed petrological and chemical study of the granitic rocks, it may be that tin and tungsten mineralizations were introduced by hydrothermal fluids that moving upward through the N-S fracture systems developed in the GM-granitic series and were trapped under the metabasites. Contemporaneously, reactions between the mineralized fluids and the wall rocks took place resulting in various kinds of wall-rock alterations such as K-feldspathization, tourmalinization, chloritization, sericitization, muscovitization, and albitization. The original source of tin and tungsten in the ore-forming fluids are still obscure. Based on higher concentrations of Sn and W in the GM-1 as compared with the GR-1 (see Tables 5, 6; Figure 12) or the world average for granites (2–3 ppm Sn, Hamaguchi and Kuroda, 1969, and probably 1–2 ppm W, Evans and Krauskopf, 1970, cited in Alderton and Moore, 1981), lead to suggest that the tin and tungsten may probably originate from the trace elements in the mineral constituents of the GM-1 granitic rocks such as biotites (Hesp, 1971; Groves 1972; Imeokparia, 1982). However, the rather high concentration of tin and tungsten in the GM-1 and the GM-2 may probably be caused by the contamination of the ore forming fluids. By analogy with similar ore deposits elsewhere, the D/H analyses on muscovites from the Mae Lama hydrothermal vein system in northwestern Thailand have proved that meteoric water is involved in the formation of primary tungsten-tin deposit (Harmon and Beckinsale, unpublished, cited in Beckinsale, 1979). Nevertheless, the original source of tin and tungsten is also still uncertain. Beckinsale (1979) questioned as to whether the interaction with meteoric water was perhaps only an extra stage in concentrating ore metals derived from the granite, or that the meteoric water that gained access to the cooling pluton contained dissolved ore components before interaction with a granite which acted only as a heat source to drive the hydrothermal circulation.

It is interesting to note that field evidences indicate that cassiterite is chiefly confined to the uppermost part of the granitic pluton, while scheelite is commonly abundant towards the lower level, and, that scheelite in the ore veins occurs at the central zone and is symmetrically salvaged by cassiterite. Furthermore, some of the cassiterite and tungsten minerals may tend to occur separately in veins. These lines of evidence lead to suggestion that tin mineralization at the Mae Chedi Mine is not contemporaneous with tungsten. It is, therefore, envisaged that tin mineralization is more intensive in the first episode of hydrothermal activity and tungsten mineralization presents a later phase. A similar finding was also obtained from the studies of tin and tungsten mineralizations at the Samoeng Mine (Punyaprasiddhi, 1980; Suensilpong and Jungyusuk, 1981). In addition, Punyaprasiddhi (1980) proposed that tin mineralization at the Samoeng Mine is more related to the Triassic granite (S-type) while tungsten mineralization represents a later mineralizing phase probably in the Cretaceous. Suensilpong and Jungyusuk (1981), again, pointed out that tin is in closer association with the porphyritic biotite granite (S-type) of Upper Triassic age, and that scheelite is related to the fine-grained biotite granites (I-type) which are younger in age and a different phase of the former granitic rock.

Scheelite deposits of northern Thailand are found mainly in contact zones between granitic rocks and calcareous rocks, e.g. Doi Mok Mine (German Geological Mission, 1972; Jivathanond, 1981), Samoeng Mine (Punyaprasiddhi, 1980), Mae Lama Mine (Suensilpong, 1975; Panupaisal, 1977; Pitragool and Panupaisal, 1979). These field evidences lead to the suggestion that the Ca in the scheelite may have originated from the calcareous country rocks. However, in the case of the Mae Chedi area, no outcrops of calcareous rocks were observed in the nearby area of the scheelite deposits. Because of the remarkable decrease in anorthite contents in plagioclases of the GM-2 and the GM-3 as compared with the GM-1 (Table 2) and some scheelite grains are spatially associated with albitic plagioclase, it would be reasonable to suspect that the major part of the Ca which is used to form scheelite may have been drawn from the formerly more calcic plagioclase of the GM-1 during the albitization. This conclusion is also supported by chemical analyses of the rocks (Tables 3, 5; Figure 8), which reveal that the CaO contents of the GM-granitic series decrease distinctively from the GM-1 to the GM-2 or the GM-3.

CONCLUSIONS

The main conclusions of this study may be summarized as follows:

1. The Mae Chedi granites consist of two granitic series (the GM- and the GR-

series) which belong to calc-alkaline, peraluminous, and the so-called S-type granitoids. Both of them are unlikely to be related to one another.

2. Hydrothermal alterations are considered to be the most likely mechanism in association with tin-tungsten related granites of the Mae Chedi area. On the contrary, the process of fractional crystallization of the main granitic phases throughout the area has not given rise to tin-tungsten mineralization. These findings may be applied not only in the study area but also elsewhere in the Khuntan Mountain Range.

3. The occurrences of tin and tungsten in the Mae Chedi Mine are primarily due to hydrothermal ore-forming fluids. The phenomena are associated with wall-rock alterations including K-feldspathization, tourmalinization, chloritization, sericitization, muscovitization, and albitization.

4. Tin and tungsten mineralizations at the Mae Chedi Mine are not contemporaneous. It is envisaged that tin mineralization is more intensive in the first episode of hydrothermal activity and tungsten mineralization represents a later phase.

5. It is likely that the major Ca which was used to form scheelite may have been derived from the pre-existing plagioclase of the GM-1 by the process of albitization.

ACKNOWLEDGEMENTS

The authors are greatly indebted to Mr. S. Changkasiri, the Director General of Department of Mineral Resources (DMR) for his kind permission to publish this paper. Thanks are due to Mr. T. Danusawad, the Director of Economic Geology Division for his full support. They are especially grateful to Dr. P. Aranyakanon, Senior Expert Geologist of DMR for his advice, and in initiating and selecting this study project, to the Chemistry Section, Geological Survey Division, DMR for chemical analysis of H_2O^+, S, Li, F, Sn, W, Cu, Pb, Zn and Ni, and to the Physics Division, office of Atomic Energy for Peace for chemical analysis of Rb, Sr, Ba, Zr, La, Ce, and U. Acknowledgements are also extended to Mr. S. Khunplin and Mr. J. Khunplin of Khunplin Mining Co., Ltd. for their hospitalities, to Mr. P. Vichit, Ms.S. Vudhichativanich, Dr. S. Nakapadungrat, Mr. P. Sukvatananunt, Mr. P. Khuenkong, and Mrs. B. Charusiri of DMR for providing information and suggestions.

REFERENCES

ALDERTON, D.H.M., and MOORE, F., 1981. New determinations of tin and tungsten in granites from south-west England. *Miner. Mag.*, 44, 354–356.

ARANYAKANON, P., 1961. *The cassiterite deposit of Haad Som Pan, Ranong province, Thailand.* Report Invest. no. 4, Roy, Dept. Mines, Bangkok, Thailand, 182 p.

BAUM, F., BRAUN, E. VON, HAHN, L., HESS, A., KOCH, K.E., KRUSE, G., QUARCH, H., and SIEBENHUNER, M., 1970. On the geologyof northern Thailand. *Geol. Jahrb.*, 102, 23 p.

————, and HAHN, L., 1977. Geological map of northern Thailand 1:250,000, Sheet 3 (Phayao). *Fed. Inst. Geosci. Nat. Res.*

BECKINSALE, R.D., 1979. Granite magmatism in the belt of south-east Asia. *In* Atherton, M.P., and Tarney, J. (Eds). *Origin of granite batholith, geochemical evidence.* Shiva publishing limited, Kent, U.K., 34–44.

BRAUN, E. VON, BESANG, C., EBERLE, W., HARRE, W., KREUZER, H. LENZ, H., MULLER, P., and WENDT, I., 1976. Radiometric age determinations of granites in northern Thailand. *Geol. Jahrb.*, 21, 171–204.

CHAPPELL, B.W., and WHITE, A.J.R., 1974. Two contrasting granite types. *Pacific Geol.*, 8, 173–174.

CHAROENPRAWAT, A., GEBERT, H., and SUKVATTANANUNT, P., 1980. *Geologic and geochemical investigati of tin deposits in Changwat Chiang Rai.* Geol. Surv. Div., Dept. Miner. Res., Bangkok, Thailand, 71 (in Thai).

CHARUSIRI, P., 1980. *Igneous complexes and tin mineralization in Phuket Island, with special reference to Chao Fa and Tor Soong Mines.* Unpub. M.Sc. thesis, Chulalongkorn Univ., Thailand, 208 p.

________, and PONGSAPICH, W., 1982. *Geology and petrochemistry of some granites of Phuket Island.* Dept. Geol., Fac. Sci. Chulalongkorn Univ., Thailand, Geol. Report no. 6, 34 p.

CHUAVIROJ, S., JUNGYUSUK, N., SUKVATTANANUNT, P., CHATURONGKAVANICH, S., CHULWONG, C., and SURIYA, S., 1978. *Geological and geochemical survey, Amphoe Mae Suai and Wiang Pa Pao, Changwat Chiang Rai.* Geol. Surv. Div., Dept. Miner. Res., Bangkok, Thailand, Unpub. Report (in Thai).

COX, K.G., BELL, J.D., and PANKHURST, R.J., 1979. *The interpretation of igneous rocks.* George Allen & Unwin, London 450 p.

GEBERT, H., SUKVATTANANUNT, P., RATTANANURUK, S., WUNAPEERA, A., 1980. *Tin and tungsten exploration in Chiang Mai and Chiang Rai provinces, northern Thailand.* Fed. Inst. Geosci. Nat. Res., Hanover, Unpub. Report no. 7, 51 p.

GERMAN GEOLOGICAL MISSION IN THAILAND, 1972. Final report. Bundesanstalt für Bodenforschung, Hannover, 94 p.

GREENLAND, L.P., 1970. An equation for trace element distribution during magmatic crystallization. *Am. Mineralogist*, 55, 455–465.

GROVES, D.I., 1972. The geochemical evolution of tin-bearing granites in the Blue Tier Batholith, Tasmanisa. *Econ. Geol*, 67, 445–457.

HESP, W.R., 1971. Correlation between the tin content of granitic rocks and their chemical and mineralogical composition, Proc. Symp. Inter. Geochem. Explor., *Canad. Inst. Mining Metall.*, Spec. 11, 341–353.

HINE, R., WILLIAMS, I.S., CHAPPELL, B.W., and WHITE, A.J.R., 1978. Contrast between I-and S-type granitoids of the Kosciusko batholith. *Jour. Geol. Soc. Australia* 25, 219–234.

HUTCHISON, C.S., 1974. *Laboratory handbook of petrographic techniques.* John Wiley & Sons, New York, 527 p.

________, 1978. Southeast Asian tin granitoids of contrasting tectonic setting. *Jour. Phys. Earth*, 26, S221–S232.

IMEOKPARIA, E.G., 1982. Tin content of biotites from the Afu younger granite complex, central Nigeria. *Econ. Geol.*, 77, 1710–1724.

ISHIHARA, S., 1977. The magnetite-series and ilmenite-series granitic rocks. *Mining Geol.*, 27, 293–305.

________, 1980. Significance of the magnetite-series and ilmenite-series of granitoids in mineral exploration, *In* Ridge, J.D. (Ed), *Proc. 5th Quadrennial IAGOD Symp.*, Germany, Schweizerbart' ische Verlagsbuchhandlung. Stuttgart, 1,309–312.

JIVATHANOND, S., 1981. *Mineralography and geochemistry of the tungsten deposits at Doi Mok, Amphoe Wiang Pa Pao, Changwat Chiang Rai.* Unpub. M.Sc. thesis, Chiang Mai Univ., Thailand, 80 p.

MAHAWAT, C., 1982. *The petrology and geochemistry of the granitic rocks of the Tak batholith, Thailand.* Unpub. Ph.D. thesis, Univ. Liverpool, U.K., 210 p.

MCCARTHY, T.S., and HASTY, R.A., 1976. Trace element distribution patterns and their relationship to the crystallization of granitic melts. *Geochim. Cosmochim.* Acta, 40, 1351–1358.

MITCHELL, A.H.G., 1977. Tectonic settings for emplacement of Southeast Asian tin granites. *Geol. Soc. Malaysia, Bull. 9,* 123–140.

NAKAPADUNGRAT, S., 1982. *Geochronology and geochemistry of the Thong-Lang granite complex, central Thailand.* Unpub. Ph.D. thesis, Univ. London, U.K., 336 p.

NEUMAN, H., MEAN. J., and VITALIANO, C.J., 1954. Trace element variation during fractional crystallization as calculated from the distribution-law. *Geochem. Cosmochim. Acta*, 6, 90–99.

NORMAN, M.B., 1974. Improved techniques for selective staining of feldspar and other minerals using amaranth. *Jour. Research U.S. Geol. Surv.*, 2, 73–79.

PANUPAISAL, S., 1977. *Mineralography and geochemistry of tungsten deposits of Mae Lama, Amphoe Mae Sariang, Mae Hong Son.* Unpub. M.Sc. thesis, Chiang Mai Univ., Thailand, 147 p. (in Thai).

PHILPOTTS, J.A., and SCHNETZLER, C.C., 1970. Phenocryst-matrix partition coefficients for K, Rb, Sr, and Ba, with applications to anorthosite and basalt genesis. *Geochim. Cosmochim. Acta*, 34, 307–322.

PITRAGOOL, S., and PANUPAISAL, S., 1979. Tin and tungsten mineralization of the Mae Lama mining district, N-W Thailand. *In* Yeap, C.H., ed., *Geology of tin deposits. Geol. Soc. Malaysia Bull. 11,* 267–281.

PLIMER, I.R., 1980. Exhalative Sn and W deposits associated with mafic volcanism as precursors to Sn and W deposits associated with granites. *Mineral. Deposita,* 15, 275–289.

PUNYAPRASIDDHI, P., 1980. *Investigation of the geology and mineralization of tin and tungsten at Samoeng Mine area north Thailand.* Unpub. Ph.D. thesis, Univ. Sheffield, U.K., 130 p.

REID, W.R., 1969. Mineral staining tests. *Miner. Indus. Bull., Colorado School of Mines,* 12, 1–20.

SCHNETZLER, C.C., and PHILPOTTS, J.A., 1970. Partition coefficients of some rare earth elements and barium between igneous matrix material and rock-forming mineral phenocrysts—I. *In* Ahrens, L.H. (Ed), *Origin and distribution of the elements.* Pergamon Press, 929–938.

SHERATON, J.W., and LABONNE, B., 1978. Petrology and geochemistry of acid igneous rock of northeast Queensland. *Bureau Miner. Res., Australia, Bull, 169,* 139 p.

STRECKEISEN, A., 1976. To each plutonic rock its proper name. *Earth Sci. Rev.,* 12, 1–33.

SUENSILPONG, S., 1975. *IGCP Circum Pacific Plutonic Project, Guide book for geological excursion to northern Thailand.* Dept. Miner. Res., Bangkok, Thailand, 7–12.

________, MEESOOK, A., NAKAPADUNGRAT, S., and PUTTHAPIBAN, P., 1977. The granitic rocks and mineralization at the Khuntan batholith, Lampang. *Geol. Soc. Malaysia, Bull. 9,* p. 159–173.

________, and JUNGYUSUK, N., 1981. *Some aspects of sheelite-related granites.* A paper presented at Symp. on Tungsten Geol., Jiangxi prov., People's Republic of China, 7 p.

TAYLOR, S.R., 1965. The application of trace element data to problems in petrology. *Phys. Chem. Earth,* 6, 133–213.

TAUSON, L.V., and KOZLOV, V.D., 1973. Distribution functions and ratios of trace-element concentrations as estimators of the ore-bearing potential of granites. *In* Jones, M.J. (Ed), *Geochemical Exploration Proc. 4th Inter. Geochem. Explo. Symp.,* London, Inst. Mining Metall., 37–44.

TEGGIN, D.E., 1975. *The granites of northern Thailand.* Unpub. Ph.D. thesis, Univ. Manchester, U.K., 198 p.

THORNTON, C.PO., and TUTTLE O.F., 1960. Chemistry of igneous rocks: I. Differentiation Index. *Am. Jour. Sci.,* 258, 664–684.

TUTTLE, O.F., and BOWEN, N.L., 1958. Origin of granite in the light of experimental studies in the system $NaAlSi_3O_8$-$KAlSi_3O_8$-SiO_2-H_2O. *Geol. Soc. Am. Mem.* 74, 153 p.

VICHIT, P., 1971. *Geological Survey of the tin deposits in Tung Kwian Teak Plantation, Amphoe Hang Chat, Changwat Lampang.* Tin Explo. Proj., Econ. Geol. Div., Dept. Miner. Res., Bangkok, Thailand, 72 p. (in Thai).

________, 1973. *Geological Survey of the tin deposits in Huai Khut and Doi Bo Kaeo, Muang Yao, Amphoe Hang Chat, Changwat Lampang.* Tin Explo. Proj., Econ. Geol. Div., Dept. Miner. Res., Bangkok, Thailand, 13 p. (in Thai).

________, 1976. *Geochemical and geological survey of tin deposits in Nam Mae Kaung-Nam Mae Lao area, Changwat Chiang Mai and Changwat Chiang Rai.* Tin Explo. Proj., Econ. Geol. Div., Dept. Miner. Res., Bangkok, Thailand, 148 p. (in Thai).

UDOMRATN, C., DHRAMMADUSDEE, V., and CHUAVIROJ, S., 1980. *Geology of Amphoe Mae Chan, Changwat Chiang Rai.* Geol. Surv. Div., Dept. Miner. Res., Bangkok, Thailand, 50 p.

Manuscript received 11th September 1984